Australian Government

Department of Defence

Defence Science and
Technology Organisation

Estimation of a Constant False Alarm Rate Processing Loss for a High-Resolution Maritime Radar System

Irina Antipov and John Baldwinson

Electronic Warfare and Radar Division
Defence Science and Technology Organisation

DSTO-TR-2158

ABSTRACT

This report addresses a problem of estimation of a constant false alarm rate (CFAR) processing loss for a high-resolution maritime radar system on an example of a generic radar system Anti-Submarine Warfare mode and discusses approaches to modelling of the detection performance for such a system. It has been shown that the value of the CFAR loss for a high-resolution radar system can vary considerably over a radar detection range, dependent on the clutter scenario and the CFAR detection processing used and, therefore, can not be given by a single number for the whole detection area, as it is usually done for a low-resolution radar system.

DSTO-TR-2158

APPROVED FOR PUBLIC RELEASE

Estimation of a Constant False Alarm Rate Processing Loss for a High-Resolution Maritime Radar System

EXECUTIVE SUMMARY

The Electronic Warfare and Radar Division (EWRD) of DSTO and BAE Australia are undertaking further software development to the Ship Air Defence Model (SADM) Modelling and Simulation Tool. One of the aims of this development is provision of detailed modelling of the performance of different detection modes of a typical maritime surveillance radar that can be installed on board a Maritime Patrol Aircraft (MPA). Note that approaches to modelling of the performance of detection modes with low range resolution are well described in scientific literature. However, approaches to modelling of the performance of detection modes with high range resolution are still very much under debate.

Automatic target detection algorithms employ constant false alarm rate (CFAR) processors to adapt a detection threshold automatically to a local background clutter and noise power in an attempt to maintain an approximately constant false alarm rate. This is achieved at the expense of a detection loss associated with the CFAR threshold setting. To predict correctly the detection performance that is achievable by a radar system in the specified conditions, it is necessary to estimate the expected value of the CFAR detection processing loss. The magnitude of this loss depends on the type of CFAR processor and the number of reference cells used, the required probability of false alarm, and the statistics of target and clutter background plus noise signals.

The CFAR loss has been extensively evaluated for several types of CFAR processors under conditions of Rayleigh amplitude backgrounds, including the effects of multiple targets and clutter edges, i.e. transitions from regions of one clutter power to another. The effects on the CFAR loss of clutter statistics deviating from the Rayleigh amplitude assumption were reported less.

This report addresses a problem of the CFAR detection processing loss estimation for a high-resolution maritime radar system in Rayleigh and non-Rayleigh backgrounds with different spatial correlation properties on an example of a generic radar system ASW mode and discusses approaches to the detection performance modelling for such a system.

It has been shown that the CFAR processing loss can vary considerably over a radar detection range, dependent on clutter scenario and the CFAR detection processing used. A simple achievable CFAR processing accuracy measure, such as the CFAR loss value that is given by a single number for the whole detection area, as it is usually done for a low-resolution radar system, is not sufficient to describe the CFAR processing loss of a high-resolution radar system expected in a complex environment. The CFAR processing loss for a high-resolution radar system must be quantified for different detection area regions and for a number of levels of complexity:

- The CFAR loss in noise-limited conditions;
- The CFAR loss in uniform clutter with changing scale and amplitude statistics (shape);
- The CFAR loss in non-uniform clutter with specified spatial characteristics (spatially correlated returns from sea swell etc).

Authors

Irina Antipov
Electronic Warfare Division

Dr. Irina Antipov is working as an EL2 S&T6 within the Radio Frequency Countermeasures Group, Electronic Warfare and Radar Division of DSTO. Her research interests are in the development of radio frequency countermeasures to airborne maritime radar systems, modelling and evaluation of naval radar systems including: investigating the performance of maritime radar systems, adapting radar systems to operate in a clutter environment, investigating concepts of operation of maritime radar systems.

John Baldwinson
Electronic Warfare Division

Mr. John Baldwinson is an EL1 S&T5 within the Maritime and Land EW Systems Group, Electronic Warfare and Radar Division of DSTO. His research interests are in the test and evaluation of maritime radar systems, the development of operation effectiveness models and the investigation of the performance of maritime radar systems in EW scenarios

Contents

1. Introduction

The Electronic Warfare and Radar Division (EWRD) of DSTO and BAE Australia are undertaking further software development to the Ship Air Defence Model (SADM) Modelling and Simulation Tool. One of the aims of this development is provision of detailed modelling of the performance of different detection modes of a typical maritime surveillance radar that can be installed on board a Maritime Patrol Aircraft (MPA). Note that approaches to modelling of the performance of detection modes with low range resolution are well described in scientific literature [2 - 9, 18, 19]. In contrast approaches to modelling of the performance of detection modes with high range resolution are still very much under debate [8, 10 - 14, 20, 23, 24, 28, 42 - 48].

In particular, the advent of high-resolution maritime radars working at low grazing angles (<10°) has introduced new problems in the area of target detection in sea clutter and its modelling. The original expectation for high-resolution radars was that with a smaller sea surface area intercepted by a narrower radar pulse, and with a lower mean clutter reflectivity corresponding to low grazing angles, the received sea clutter would be less, leading to a significant detection improvement. It turns out that this improvement is not as great as was expected since high-resolution and/or low grazing angle sea clutter statistics are no longer Rayleigh and target-like sea spikes are introduced in the radar return signal. These increase the number of false alarms, necessitating higher threshold settings that make the detection of small targets in spiky sea clutter more difficult.

To adapt a detection threshold automatically to a local background clutter and noise power in an attempt to maintain an approximately constant false alarm rate, radars employ constant false alarm rate (CFAR) processors. This is achieved at the expense of a detection loss associated with the CFAR threshold setting. The magnitude of this loss depends on a type of CFAR processor and a number of reference cells used, required probability of false alarm, and, more importantly, on statistics of target and clutter plus noise background signals [1-20, 23, 24, 28, 42 - 48].

The CFAR loss has been extensively evaluated for several types of CFAR processors under conditions of Rayleigh amplitude backgrounds, including the effects of multiple targets and clutter edges, i.e. transitions from regions of one clutter power to another. The effects on the CFAR loss of clutter statistics deviating from the Rayleigh amplitude assumption are not reported as often.

This report addresses a problem of the CFAR loss estimation for a high-resolution maritime radar system in Rayleigh and non-Rayleigh backgrounds with different spatial correlation properties on a generic radar system Anti-Submarine Warfare (ASW) mode, which would be used for detection of small surface targets, e.g. exposed periscopes.

2. Target Model and Radar Specification for a Generic ASW Mode

2.1 Target Model

To represent periscope radar returns received by the ASW mode, a simple, physically motivated model of the radar signature of a periscope in the sea viewed from low grazing angles (≤4°), proposed by Tonkin and Dolman [41], is used in the report.

The periscope is assumed to be a metal cylinder of known dimensions, and the following effects are incorporated in its radar return modelling:

- Shadowing of the periscope by the sea surface,

- Specular multipath,

- Much higher power of the return when the periscope is orthogonal to the line of sight of the radar due to a lobe structure of the backscatter return from a cylinder in elevation,

- Additional component of the return produced by an approximately orthogonal corner reflector formed by the nearly vertical periscope and the sea surface.

According to the accepted model, if a radar with frequency agility is used, mostly the periscope return is uncorrelated from pulse to pulse and its fast fluctuating RCS can be described by a Chi-distributed probability density function (PDF) with 2 degrees of freedom (i.e. by a Rayleigh PDF), although there are occasional periods when a much higher return is received [41].

Hence, the largest expected value of the CFAR processing loss corresponds to the case when the periscope behaves as a simple Swerling 2 target, and the major attention in the report is paid to the CFAR processing loss estimation when detecting a small target that is well described by a Swerling 2 model.

2.2 Radar Specification for a Generic ASW Mode

The CFAR processing design that is employed in a generic ASW mode of a maritime radar system has to maintain the required probabilities of false alarm and detection, of a submarine periscope with a given RCS for sea clutter characteristics observed in specified sea state conditions, while adhering to a specified scan regime.

A statement of work for a high-resolution maritime radar ASW system detecting a submarine periscope may be formulated as follows: 'The radar system shall be capable of automatically detecting with a probability of detection of 0.5 and a false alarm rate of 1 in 30 minutes or less a submarine periscope with the radar cross section (RCS) of 1 square metre, moving with the velocity of up to 20 knots and exposed for 12 seconds or less, at up to and including a range of 32 nautical miles, in sea state up to and including 3, when scanning the 360° azimuth coverage of the radar system at altitudes up to and including 1000 feet".

The following specification, presented in Table 1, is typical of a maritime radar ASW mode, which may be installed into a maritime patrol aircraft with the aim to detect such targets.

Table 1: Specification of a generic airborne maritime surface search radar ASW mode.

Parameter	Value/Description
Centre Frequency, GHz	9.5
Mean Transmitter Power, Watts	250
Coherent	Yes
Pulse Compression	Linear Chirp
Frequency Agility Bandwidth, MHz	400 (sequenced)
Bandwidth (instantaneous), MHz	100
Range Resolution, m	2.5
Range Sidelobes, dB	Peak: -28; Integrated: -15
Polarisation	Horizontal
Scan Rate (continuous rotation), Rpm	40
Field of Regard, Degrees	360
PRF, kHz	2
Antenna Azimuth Beamwidth, Degrees	1.2
Azimuth Sidelobes	Peak: -30; Integrated: -15
Antenna Vertical Beamwidth, Degrees	5
Antenna Vertical Beamshape	Gaussian
Antenna Gain, dB	36
Receiver Noise Factor, dB	5
Additional System Losses, dB	~ 4
Processing Losses (excluding CFAR loss), dB	~ 4
False Alarm Rate Reduction	Generic "4 out of 7"
Instrumented Range, nmi	1 to 40

2.2.1 Required Probability of False Alarm

The statement of work specifies a requirement to CFAR processing that there must only be a single false alarm (false detection) in any thirty-minute period. This top-level specification for false alarm rate is easily related to the equivalent probability of false alarm within a radar detection cell ($\overline{P}_{faOUT}$) after scan-to-scan processing and then to an equivalent probability of false alarm within a range cell ($\overline{P}_{faIN} = \overline{P}_{fa}$) at the input to the scan-to-scan processor [1 – 4].

The probability of false alarm at the output of the scan-to-scan integrator of the detection modes is calculated based on the range extent, the range cell resolution, the

antenna azimuth beamwidth, the scan area size and the mode scan rate, and is given by

$$\overline{P}_{faOUT} = \frac{R_M * \Delta\theta}{R_T * 1852 * V_{scan} * \Delta T_{FA} * 360}$$

(3.1)

where R_T is the range extent of the mode (nm), 1852 is the conversion of nm to m, V_{scan} is the mode scan rate (rotations per minute); ΔT_{FA} is the required false alarm rate, 1 in ΔT Min; R_M is the range cell resolution (m), $\Delta\theta$ is the azimuth beamwidth (degrees), 360 is the full scan area size (degrees).

The probability of false alarm $\overline{P}_{faIN}$ required at the input of the scan-to-scan integrator in order to achieve the required $\overline{P}_{faOUT}$ must be calculated based on the analysis of the final stage of processing to be applied before a target is declared – the scan-to-scan integration procedure. If designed correctly, the scan-to-scan integrator will provide a large decrease in the false alarm rate with minimal effect on the probability of detecting a target. The design of a scan-to-scan integrator is complicated by the potential for a target to move through range resolution bins over the period that integration is being performed. This forces the designer of the integrator to employ a velocity banding technique which tests for a pattern of detections in a neighbourhood of resolution cells over several scans which is consistent with a range of possible target velocities.

It can be shown that for the combined "track-while-scan" and "*m* out of *n*" scan-to-scan integration procedure [5, 9], that is usually implemented in a generic ASW mode, the output false alarm rate $\overline{P}_{faOUT\ T}$ in a single velocity band, is related to the input false alarm rate by

$\overline{P}_{faOUT}$ = *(Probability of m hits out of n scans)*

   = *(Probability of a false alarm in the test range cell) * (Probability of a false alarm*

   in (m-1) out of the (n-1) subsequent scans laying in a single velocity band)

$$= \overline{P}_{faIN}\ \left\{ \alpha\ \ C_{m-1}^{n-1}\ \ \overline{P}_{faIN}^{m-1}\ \ \left(1 - \overline{P}_{faIN}\right)^{m-1} \right\}$$

(3.2)

where:

  $\overline{P}_{faIN}$ is the probability of false alarm at the input of scan -to-scan integrator,

  which is equal to probability of false alarm within each range cell,

  C_{m-1}^{n-1} is the combinatorial for groupings of (*m*-1) out of (*n*-1),

  α is the factor to allow for the number of range cells within the (*n*-1) subsequent scans, which can contribute to detection in a particular velocity band.

Assume that the implementation of the scan-to-scan integrator with the "track before detect" procedure will result in an effective performance identical to a "4 out of 7" integrator

$$\overline{P}_{faOUT} = \text{(Probability of 4 hits out of 7 scans)} = \tag{3.3}$$

$$= \sum_{k=4}^{7} \binom{7}{k} * \left[\overline{P}_{faIN}\right]^k * \left[1 - \overline{P}_{faIN}\right]^{7-k} = 35 * \overline{P}_{faIN}^4 - 84 * \overline{P}_{faIN}^5 + 70 * \overline{P}_{faIN}^6 - 20 * \overline{P}_{faIN}^7$$

The reduction in false alarm rate afforded by this type of integrator is shown in Figure 1.
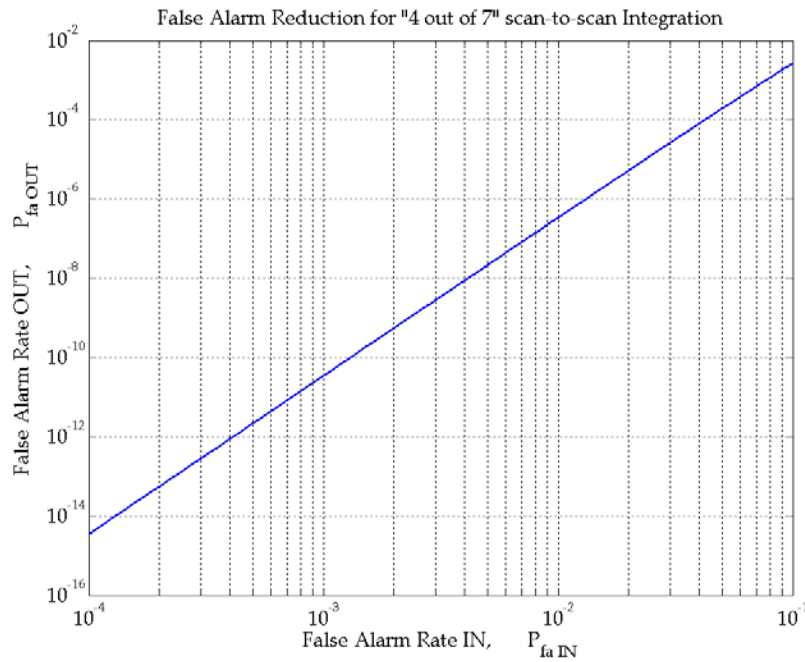
Figure 1: False alarm rate reduction from "4 out of 7" binary integration.

A straight-line approximation to (3.3) has been derived as

$$\overline{P}_{faOUT} = 10^{4.348 \log_{10} \overline{P}_{faIN} + 2.538} \tag{3.4}$$

Hence, the $\overline{P}_{faIN} = \overline{P}_{fa}$ can be calculated as

$$\overline{P}_{faIN} = 10^{0.23 * (\log_{10} \overline{P}_{faOUT} - 2.538)} \tag{3.5}$$

Thus, in order to achieve the false alarm rate of 1 in 30 minutes or less for the ASW mode with the parameters specified in Table 1, a chosen CFAR processing design has to provide the average probability of false alarm within a range cell at the input to the scan-to scan processor that is equal to $\overline{P}_{fa} = 2.44 * 10^{-5}$ or less.

2.2.2 Required Probability of Detection

The statement of work also specifies a requirement to CFAR processing that the average probability of detection after scan-to-scan integration has to be $\overline{P}_{dOUT} \geq 0.5$. The $\overline{P}_d$ after scan-to-scan integration for a generic ASW detection mode (for a binary integration with "4 out of 7" second threshold) is given by formula [1 - 4]

$$\overline{P}_{dOUT} = \sum_{k=4}^{7} \binom{7}{k} * \left[\overline{P}_d\right]^k * \left[1 - \overline{P}_d\right]^{7-k} = 35\overline{P}_d^4 - 84\overline{P}_d^5 + 70\overline{P}_d^6 - 20\overline{P}_d^7 , \qquad (3.6)$$

where $\overline{P}_d$ is the average probability of detection in each scan.

Figure 2 presents the relationship between $\overline{P}_{dOUT}$ after "4 out of 7" scan-to-scan integration and single scan $\overline{P}_d$ for the analysed ASW mode design.
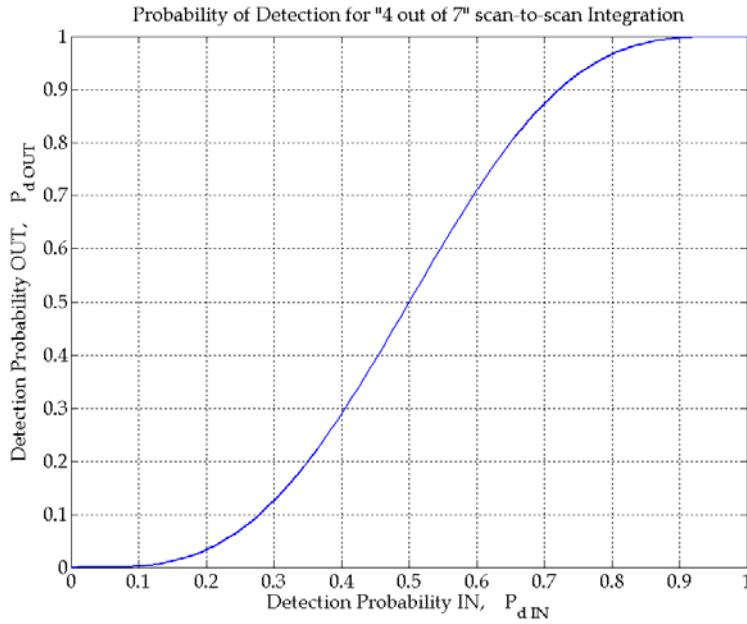
Figure 2: Relationship between $\overline{P}_{dOUT}$ after scan-to-scan integration versus the single scan $\overline{P}_d$ for the analysed ASW mode design ("4 out of 7").

It can be seen that for the ASW mode design that uses "4 out of 7" scan-to-scan processor, this requirement is met only if the average probability of detection achieved in a single scan is $\overline{P}_d \geq 0.5$. Therefore, the required average probability of detection in a single scan $\overline{P}_d$ is 0.5.

In order to simultaneously meet these tough requirements for probabilities of false alarm and detection when detecting such a small target in complicated maritime

environment, the CFAR design must achieve a compromise between producing a low CFAR loss and providing the ability to adapt to rapidly changing clutter.

3. CFAR Loss Estimation for a Generic ASW Mode with Basic Design CFAR Processors

To estimate a CFAR loss that a high-resolution maritime radar system with the specified parameters has in certain environmental conditions, it is necessary to:

- Analyse sea clutter statistical properties (such as amplitude distribution, spatial and temporal correlation functions) that are observed in these conditions,

- Consider the best (i.e. "ideal") detection performance that such a system can achieve on assumption that the sea clutter plus noise amplitude distribution parameters are explicitly known, and then

- Predict a loss that is introduced by a CFAR processor implemented in the system in order to estimate parameters of the sea clutter plus noise amplitude distribution and clutter-to-noise ratio (*CNR*) unknown in practice.

The following sections of the report present the results of the CFAR loss estimation for a generic radar system ASW mode in Rayleigh and non-Rayleigh backgrounds with different spatial correlation characteristics for three basic design CFAR processors that use:

- Either the "cell-averaging", or "greatest of", or "smallest of" logic for the estimation of the mean level of the sea clutter plus noise amplitude distribution, and

- A number of different algorithms for the estimation of this distribution variance (which is calculated from the shape parameter).

3.1 Statistical Model of High-Resolution Sea Clutter plus Noise Mixture

It is well known that for radar modes, in which the resolution cell dimensions are much greater than the swell wavelength, and for grazing angles greater than about 10°, the clutter amplitude is Rayleigh distributed.

When the radar resolution is improved and/or for smaller grazing angles, as it is for the generic ASW mode, the clutter amplitude distribution is observed to develop a longer tail (i.e. higher number of amplitude values much greater than the mean value) and the returns are often described as becoming "spiky".

The statistical results of many experiments in recent years [1-20, 23, 24, 28, 42 - 48] provide evidence that the K-distribution is the most appropriate model for such sea clutter in the low *Pfa* region. This is a two parameter distribution, characterised by a shape parameter, *v*, and a scale parameter, *b*.

For a square-law detector, the PDF of the K-distributed sea clutter envelope, x, is [13]

$$p(x) = \int_0^\infty p(x/y)p(y)dy = \frac{2c^{\nu+1}}{\Gamma(\nu)} x^{\frac{\nu-1}{2}} K_{\nu-1}(2c\sqrt{x}), \qquad (3.7)$$

$$p(x \mid y) = \frac{\pi}{4y^2} \exp\left(-\frac{\pi x}{4y^2}\right), \qquad (0 \le x \le \infty) \qquad (3.8)$$

and

$$p(y) = \frac{2b^{2\nu}}{\Gamma(\nu)} y^{2\nu-1} \exp\left(-b^2 y^2\right), \qquad (0 \le y \le \infty) \qquad (3.9)$$

where $4y^2/\pi$ represents the underlying mean intensity of clutter, which may vary spatially and temporally, $c = b\sqrt{\pi/4}$, $K_\nu(x)$ is a modified Bessel function, and $b^2 = \dfrac{\nu}{\overline{y}^2}$, where $\overline{y}^2$ is the average power of clutter.

The main advantage to using the K-distribution for modelling of the sea clutter is that it not only describes the amplitude statistics, but takes into account the temporal and spatial correlation properties of the sea clutter as well. In its compound form, (3.1), the K-distribution model is decomposed into two components [1-20, 23, 24, 28, 42 - 48].

Thus, the first component in (3.7) is the local mean level, y, obeying a generalised Chi-distribution (3.9). This local mean level has a long temporal de-correlation period on the order of a few seconds and it is not affected by frequency agility. The second component in (3.7), x, is called the speckle. This component is Rayleigh distributed, (3.28), and has a mean level determined by the first component of the model. The speckle has a short temporal de-correlation period on the order of tens of milliseconds, and can be de-correlated from pulse to pulse by frequency agility. These two components are in good agreement with experimental results; therefore the model provides an appropriate representation of sea clutter correlation properties.

Thermal noise in the radar receiver, which in general cannot be neglected, modifies the distribution of the received signals. In the presence of noise, the speckle component of the sea clutter return is effectively modified by an increase in its average power. The new speckle component can be determined as having the Rayleigh distribution of [13, 42 - 48]

$$p(w \mid y) = \frac{1}{(2\sigma^2 + (4y^2/\pi))} \exp\left(-\frac{w}{(2\sigma^2 + (4y^2/\pi))}\right), \qquad (3.10)$$

where w is the overall clutter plus noise return and $2\sigma^2$ is the noise power level.

The distribution of K-distributed clutter combined with additive thermal noise is not K-distributed and a closed-form expression defining this distribution function does not exist [13, 27, 37, 42 - 48]

$$p(w) = \int_{0}^{\infty} \frac{1}{(2\sigma^2 + (4y^2/\pi))} \exp\left(-\frac{w}{(2\sigma^2 + (4y^2/\pi))}\right) \frac{2b^{2\nu}}{\Gamma(\nu)} y^{2\nu-1} \exp\left(-b^2 y^2\right) dy, \quad (3.11)$$

The average *CNR*

$$CNR = \frac{4}{\pi b^2} \frac{\nu}{2\sigma^2} = \frac{2}{\pi} \frac{\bar{y}^2}{\sigma^2}. \tag{3.12}$$

Then, if the received data has a low *CNR* (say, *CNR* < 10dB), the resulting amplitude distribution will be significantly altered from a standard K-distribution and the low amplitude values of the clutter amplitude distribution will be the most affected by this noise [27, 37, 42 - 48].

3.2 Ideal Detection Performance Assessment for a High-Resolution Maritime Radar System

The conventional approach to "ideal" performance assessment for any radar system is to consider an "ideal fixed" threshold, adjusted to give the required overall *Pfa* [1, 27, 28, 31, 42]. When such a threshold is applied above the estimated "global" mean clutter plus noise level, the *Pfa* and *Pd* vary with a local value of the mean clutter level *y* and, hence, vary temporally and spatially.

Recent research into a high-resolution maritime system detection performance in sea clutter has shown [27, 42 - 48], however, that in some cases it may be possible for the threshold to adapt to the "local" mean clutter level and, thus, provide a value of *Pfa*, which does not vary spatially. When this adaptation is achieved perfectly, the detection performance is termed "ideal CFAR".

As both "ideal fixed" and "ideal CFAR threshold settings can be used as a baseline for comparison with real system detection performances, each of them will be considered in more detail.

3.2.1 "Ideal Fixed" Threshold Detection

For "ideal fixed" threshold detection of single pulse K-distributed strong clutter returns, when *b* and *ν* are known a priori and noise can be neglected, the *Pfa* is given by the cumulative distribution of *x*:

$$\left(\bar{P}_{fa}\right)_{ideal\ fixed} = \frac{2}{\Gamma(\nu)}\left(\frac{t\nu}{\mu}\right)^{\nu/2} K_\nu\left(2\sqrt{\frac{t\nu}{\mu}}\right) = \frac{2}{\Gamma(\nu)}\left(\beta_{ideal\ fixed}\nu\right)^{\nu/2} K_\nu\left(2\sqrt{\beta_{ideal\ fixed}\nu}\right), \tag{3.13}$$

where t is the detection threshold, $\mu = \bar{x}$ is the mean clutter level, and $\beta_{ideal\ fixed}$ is the threshold-multiplying factor :

$$\beta_{ideal\ fixed} = \frac{t}{\mu} = \frac{\nu\ t}{c^2} = \frac{4\nu\ t}{\pi\ b^2}\ . \tag{3.14}$$

Therefore, if clutter is known to be much stronger than noise and K-distributed, and accurate estimates of ν and b (or μ) are available, then an appropriate threshold can be set to provide the required *Pfa* by using (3.14) to determine the value of threshold-multiplying factor $\beta_{ideal\ fixed}$.

The overall *Pd* for "ideal fixed" threshold detection of a Swerling 2 target in single pulse dominantly K-distributed sea clutter return is given by

$$\left(\overline{P}_d\right)_{ideal\ fixed} = \int_0^\infty \frac{2b^{2\nu}}{\Gamma(\nu)}\ y^{2\nu-1}\exp\left(-b^2 y^2\right)\exp\left(-\frac{\beta_{ideal\ fixed}\ \mu}{4y^2\big/\pi + \overline{A}^2}\right)dy\ , \tag{3.15}$$

where $\overline{A}^2$ is the mean square amplitude of a Rayleigh distributed fluctuating target such as the average signal to clutter plus noise ratio (*S(C+N)R*) is given by

$$S(C+N)R = \frac{\overline{A}^2}{\overline{w}^2} = \frac{\overline{A}^2}{2\sigma^2 + (4\bar{y}^2\big/\pi)}\ . \tag{3.16}$$

For "ideal fixed" threshold detection of single pulse K-distributed clutter returns combined with non-negligible noise, when b, ν and σ^2 are known a priori, the *Pfa* is given by the cumulative distribution of w (3.11):

$$\left(\overline{P}_{fa}\right)_{ideal\ fixed} = P(w > t) = \int_0^\infty \exp\left(-\frac{t}{2\sigma^2 + (4y^2\big/\pi)}\right)\frac{2b^{2\nu}}{\Gamma(\nu)}\ y^{2\nu-1}\exp\left(-b^2 y^2\right)dy =$$

$$= \frac{2}{\Gamma(\nu)}\left[\frac{\nu}{\bar{z}}\frac{CNR}{(1+CNR)}\right]^\nu \int_0^\infty \exp\left(-\frac{\beta_{ideal\ fixed}\ \bar{z}}{\dfrac{\bar{z}}{CNR+1} + \dfrac{4y^2}{\pi}}\right)y^{2\nu-1}\exp\left[-\frac{\nu}{\bar{z}}\frac{CNR}{(1+CNR)}y^2\right]dy \tag{3.17}$$

where $\bar{z}$ is the mean clutter plus noise level:

$$\bar{z} = \frac{4\bar{y}^2}{\pi} + 2\sigma^2 = \mu + 2\sigma^2 = \mu\left(1 + \frac{1}{CNR}\right)\ . \tag{3.18}$$

From (3.17), it can be seen that a closed-form expression defining the overall *Pfa* does not exist. In this case, if the clutter is known to be K-distributed and accurate estimates of ν, b and σ^2 (or *CNR*) are available, the required *Pfa* is achieved by setting above the

estimated clutter plus noise level an appropriate threshold-multiplying factor $\beta_{ideal\ fixed}$ that has to be determined by numerically solving (3.17).

Then the overall Pd for "ideal fixed" threshold detection of a Swerling 2 target in single pulse K-distributed clutter returns combined with noise is determined as

$$\left(\overline{P}_d\right)_{ideal\ fixed} = \int_0^\infty \frac{2b^{2\nu}}{\Gamma(\nu)} y^{2\nu-1} \exp\left(-b^2 y^2\right) \exp\left(-\frac{\beta_{ideal\ fixed}\ \overline{z}}{2\sigma^2 + 4y^2/\pi + \overline{A}^2}\right) dy \ , \qquad (3.19)$$

However, it was shown [13, 27, 42 - 48] that a reasonable guide to the "ideal fixed" threshold radar performance prediction for single pulse detection, is to represent the received signal, which is a mixture of K-distributed sea clutter with a shape parameter ν and non-negligible noise, as being K-distributed with a modified effective shape parameter ν_{eff}:

$$\nu_{eff} = \nu\left(1 + \frac{1}{CNR}\right)^k = \nu\left(1 + \frac{2\sigma^2}{4\bar{y}^2/\pi}\right)^k \approx \nu\left(1 + \frac{1}{CNR}\right)^2 , \qquad (3.20)$$

where for single pulse detection in each scan

$$k = \begin{cases} 2.25 - 0.123n & for\ Swerling\ 2\ target \\ 2.27 - 0.135n & for\ Swerling\ 0\ target \end{cases} , \qquad (3.21)$$

$$n = -\log_{10}\left(P_{fa}\right).$$

This approximate approach to detection in clutter plus noise mixture allows using detection curves for clutter alone. Then, the overall Pfa and Pd of Swerling 2 target for "ideal fixed" detection in single pulse K-distributed clutter returns combined with non-negligible noise are approximately given as [13, 27, 42 - 48]

$$\left(\overline{P}_{fa}\right)_{ideal\ fixed} \approx \frac{2}{\Gamma(\nu_{eff})}\left(\beta_{ideal\ fixed}\nu_{eff}\right)^{\nu_{eff}/2} K_{\nu_{eff}}\left(2\sqrt{\beta_{ideal\ fixed}\nu_{eff}}\right), \qquad (3.22)$$

$$\left(\overline{P}_d\right)_{ideal\ fixed} \approx \int_0^\infty \frac{2b^{2\nu_{eff}}}{\Gamma(\nu_{eff})} y^{2\nu_{eff}-1} \exp\left(-b^2 y^2\right) \exp\left(-\frac{\beta_{ideal\ fixed}\ \mu}{4y^2/\pi + \overline{A}^2}\right) dy \ , \qquad (3.23)$$

For single pulse detection this method is accurate to within about ±1dB for $10^{-2} \le \overline{P}_{fa} \le 10^{-7}$, $0.1 \le \overline{P}_d \le 0.9$ and $0.2 \le \nu \le 10$.

3.2.1.1   Detection Regions

It is well known that the detection performance of any maritime system can be characterized by three detection regions [38, 39]:

1. The clutter-limited region, where the calculated threshold multiplier value in clutter plus noise mixture is within 1dB of the asymptotic threshold multiplier value in clutter alone. In this region, statistical characteristics of clutter and noise mixture (such as the amplitude PDF characteristics, temporal and spatial correlation properties) are determined by clutter, and the achieved *Pfa* and *Pd* are determined mostly by the clutter statistical properties.

2. The intermediate region, where the calculated threshold multiplier value in clutter plus noise mixture is neither within 1dB of the asymptotic threshold multiplier value in clutter alone nor within 1dB of the asymptotic threshold multiplier value in noise alone. In this region the statistical characteristics of clutter and noise mixture have a strong influence on the detection performance. The achieved *Pfa* and *Pd* are dependent not only on the clutter statistical properties, but on a particular value of *CNR*.

3. The noise-limited region, the calculated threshold multiplier value in clutter plus noise mixture is within 1dB of the asymptotic threshold multiplier value in noise alone. In this region the statistical characteristics of the clutter and noise mixture are determined by statistical characteristics of noise alone.

An empirical fit to the required "ideal threshold" multiplier β value (i.e. the required $S(C+N)R_{REQ}$) for achieving a desired *Pfa*, as a function of the *CNR* and the clutter shape parameter ν, was proposed in [31]

$$S(C+N)R_{REQ} = \frac{SNR_{REQ} + CNR\sqrt{\dfrac{4\bar{y}^2/\pi}{4\bar{y}^2/\pi + 2\sigma^2 \nu}} * SCR_{REQ}}{1 + CNR\sqrt{\dfrac{4\bar{y}^2/\pi}{4\bar{y}^2/\pi + 2\sigma^2 \nu}}} \, , \tag{3.24}$$

where SNR_{REQ} is the required threshold multiplier value for achieving a desired *Pfa* in the absence of clutter and SCR_{REQ} is the required threshold multiplier in the absence of noise.

As an example, Figure 3 presents the required $S(C+N)R_{REQ}$ values for achieving $\bar{P}_{fa} = 10^{-6}$ for "ideal fixed" threshold detection as a function of the *CNR* and different values of clutter shape parameter ν [31].
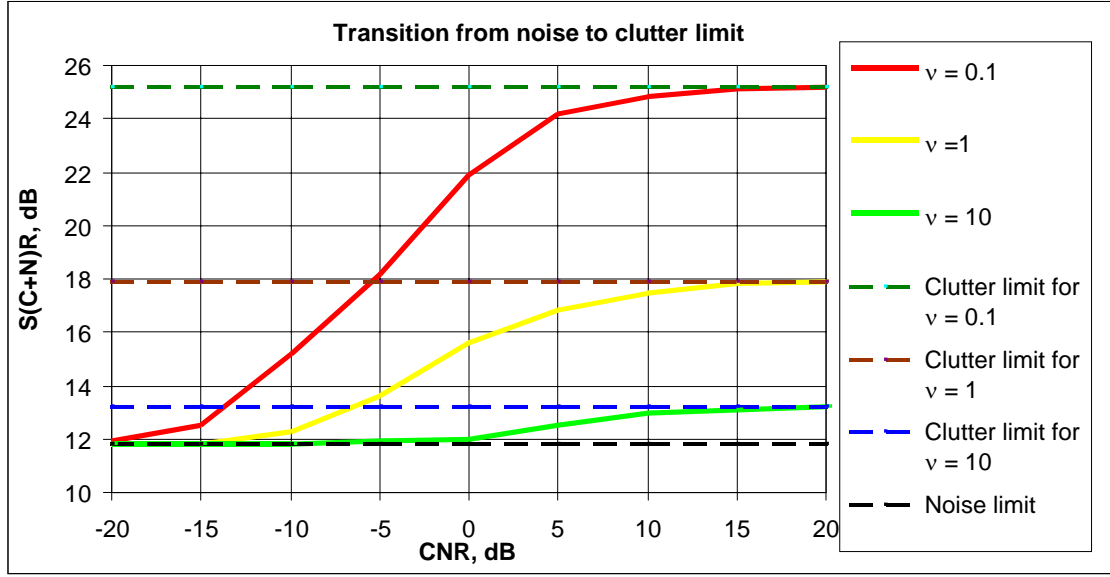
Figure 3: Transition of the threshold multiplier from noise- to clutter-limited interference for $\overline{P}_{fa} = 10^{-6}$.

Thus, for a given *Pfa*, the boundaries of the three detection regions are determined only by the clutter shape parameter ν and the *CNR* (i.e. by the amount of energy reflected from the sea surface and the ASW mode noise power) [1, 13, 24, 31, 32, 38].

Consider in more detail each of them.

3.2.1.2   Shape Parameter Prediction

The expected shape parameter ν value of the K-distributed clutter amplitude PDF can be predicted for a generic radar system ASW mode by an empirical formula that consists of the shape parameter dependence on the radar look direction relative to the swell direction [1, 25, 30]

$$\log_{10}(\nu) = \frac{2}{3}\log_{10}(\varphi) + \frac{5}{8}\log_{10}(L_c) + \frac{5}{8}\log_{10}\left(\frac{\Delta R}{4}\right) - K_p - K_S\left[\frac{1}{3}\cos(2\theta_{sw})\right], \qquad (3.25)$$

where:

   φ is the grazing angle (deg),

$$\varphi = \sin^{-1}\left((2R_e h_s + h_s^2 - R_s^2)/(2R_s R_e)\right),$$

   h_S is the height of sensor (the aircraft altitude) (m),

   R_s is the slant range (m): $R_s = \sqrt{R^2 + h_s^2}$,

   R is the current range (m),

R_e is the 4/3 radius of the earth (m).

L_c is the cross range resolution: $L_c = \Delta\theta\, R$,

$\Delta\theta$ is the azimuth beamwidth (rad),

ΔR is the range resolution (m),

K_p describes the polarisation effect:

$$K_p = \begin{cases} 1 & for \quad vertical \quad polarisation \\ 1.7 & for \quad horizontal \quad polarisation \end{cases},$$

K_S takes into account swell influence:

$$K_S = \begin{cases} 1 & if \quad swell \quad is\ observed \\ 0 & if \quad swell\ is\ not \quad observed \end{cases},$$

θ_{sw} is the angle between the boresight and the swell direction (the angle is zero when the boresight is pointed in the swell direction).

The main conclusions from the analysis of this empirical model for the shape parameter are:

1. For horizontal polarisation the value of the shape parameter is lower than for the vertical polarisation for the same set of environmental and radar parameters. It means that with horizontal polarisation, the clutter is spikier and pulse-to-pulse correlation is greater than with vertical polarisation in similar conditions.

2. Aspect angle variation depends on the swell and long wavelength sea wave content of sea spectrum: smaller values of the shape parameter are characterised for up and down swell directions, larger values are usual for across swell direction and medium values of the shape parameter are typical for the intermediate directions.

3. At different ranges, the cross-range patch size is different due to the antenna footprint, and there is a strong trend for increased values of the shape parameter with increased patch size.

4. A small grazing angle implies smaller shape parameter.

5. There is no strong statistical trend with sea state, wind speed or aspect angle relative to the wind direction.

Figures 4 and 5 present the sea clutter amplitude distribution shape parameter values for a generic radar system ASW mode with the chosen design in all radar look directions relative to the wind direction for the specified conditions of sea state 3 and flying altitude of 1000 ft. Figure 4 presents the shape parameters for the case when swell is not observed. Figure 5 presents the shape parameters for the case of a fully developed sea (i.e. when swell is observed and the swell direction is the same as the wind direction).

It can be seen that, for the case when swell is not observed, the shape parameter values reduce with range in a similar fashion for all radar look directions relative to the wind direction: the highest values of the shape parameter (0.5 - 0.6) correspond to close ranges, and the smallest values (0.2 – 0.3) – to far ranges. For the case of a fully developed sea, the change in the shape parameter values depends strongly on the radar look direction relative to the swell direction: the highest values of the shape parameter (1.2 – 1.4) correspond to close ranges and cross-swell radar look directions, and the smallest values (0.1 – 0.3) – to far ranges and up/down swell look directions.

Knowing the expected values of the sea clutter shape parameter, for a given *Pfa,* it is possible to determine the *CNR* values corresponding to the boundaries for the clutter-limited, intermediate and noise-limited detection regions for all look directions relative to the wind/swell direction using (3.24).

Thus, for the desired $\overline{P}_{fa} = 2.44 * 10^{-5}$, chosen ASW mode parameters and the shape parameter values observed for the flying altitude of 1000 ft, the *CNR* values corresponding to the boundaries of the three detection regions can be determined as follows:

- The noise-limited detection region corresponds approximately to the detection ranges for which the *CNR* < -15dB.

- The intermediate detection region corresponds approximately to the detection ranges for which – 15dB < *CNR* < 10dB.

- The clutter-limited region corresponds approximately to the detection ranges for which the *CNR* > 10dB.
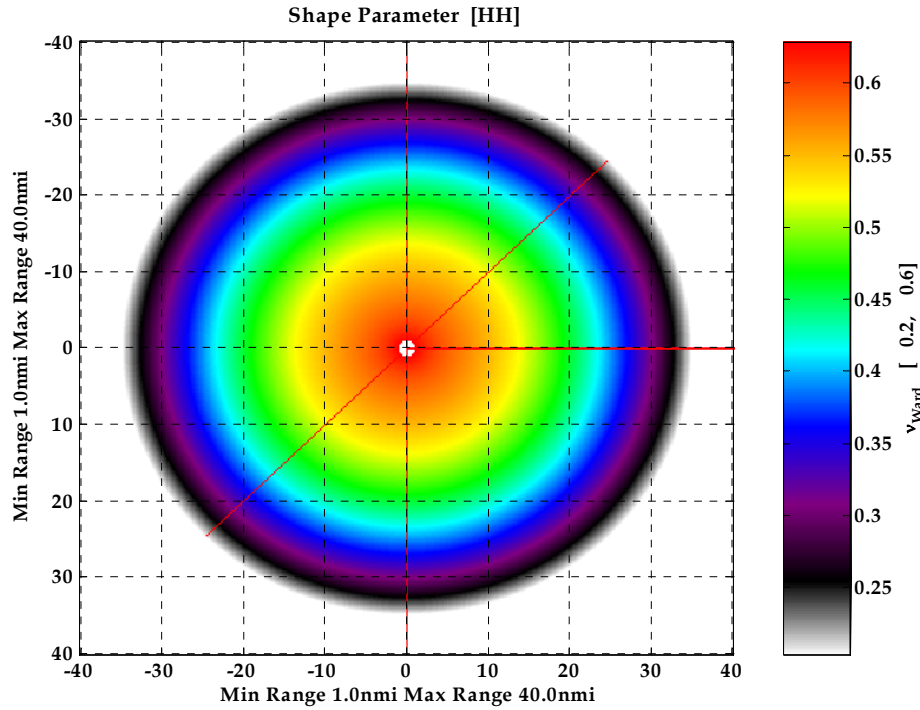
Figure 4: Shape parameters in all look directions compared to the wind direction in conditions of a sea state 3, when swell is not observed. The wind is coming from the top of the diagram. Horizontal polarisation.
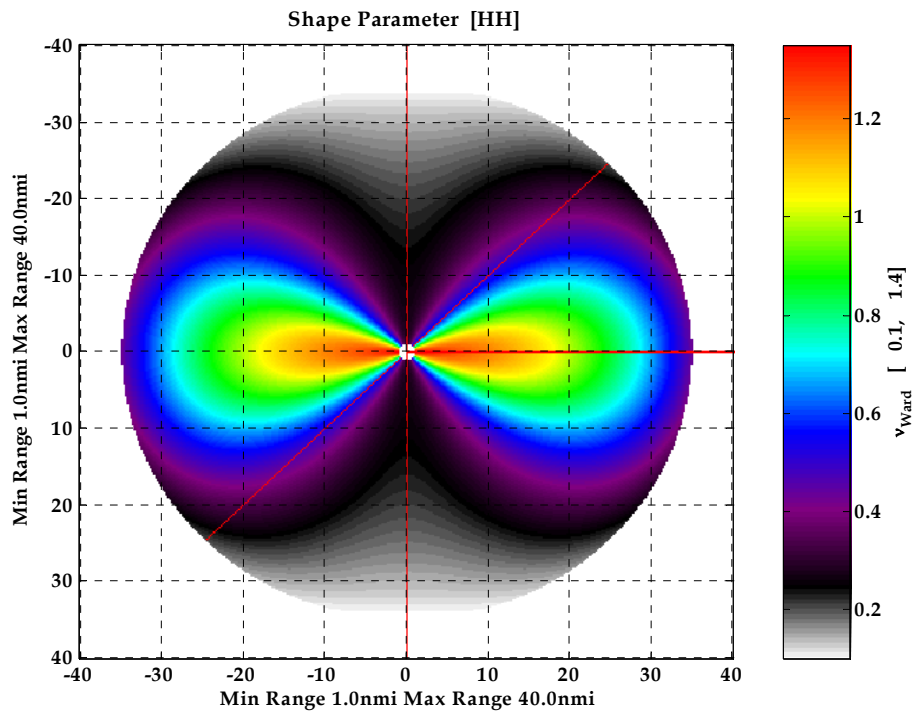
Figure 5: Shape parameters in all look directions compared to the wind/swell direction in conditions of a sea state 3, when swell is observed, and the swell direction is the same as the wind direction. The wind/swell is coming from the top of the diagram. Horizontal polarisation.

3.2.1.3   Clutter to Noise Ratio Prediction

The *CNR* for any particular range and radar look direction relative to the wind direction has to be predicted using the standard radar equation for area clutter, which takes into account the ASW mode parameters (frequency, noise temperature, range resolution, two-way antenna azimuth beamwidth and the ASW mode gains and losses applied to sea clutter processing), the aircraft flying altitude, and the mean clutter reflectivity value corresponding to the range and radar look direction relative to the wind direction [1 - 4]

$$CNR = \frac{P_t \, G_a^2 \, \sigma_c \, \lambda^2 \, G_p \, L_{cl}}{(4\pi)^3 \, R_s^4 \, k_B \, T_s \, B_n}$$
(3.26)

where

P_t is the transmitter peak power,

G_a is the antenna gain,

σ_c is the clutter RCS: $\sigma_c = \sigma_0 A_c = \sigma_0 \, R \, \theta_2 \, \Delta R$,

σ_0 is the mean clutter reflectivity,

A_c is the area of the cluttered cell,

θ_2 is the two-way azimuth beamwidth,

λ is the radar wavelength,

k_B is the Boltzman's constant,

T_s is the system noise temperature,

B_n is the mode noise bandwidth,

G_p is the mode pulse compression gain,

L_{cl} is the mode total loss applied to clutter reflected signals:

$$L_{cl} = L_{prop} L_{el} L_{mism},$$

L_{prop} is the propagation loss that depends on range. For the flight altitude of 1000ft, the propagation loss (in dB) is given by:

$L_{prop}(dB) = -0.0444R(nm)$,

R(nm) is range to the target in nautical miles.

L_{mism} is the mode pulse compression mismatch loss,

L_{el} is the mode elevation pattern loss that given by

$$L_{el} = Elloss(\theta) = 40\log_{10}(abs(f(\theta)),$$

f (θ) is the antenna pattern factor that denotes a one-way voltage ratio.

Table 2 presents typical values of processing gains and losses for a generic ASW mode that shall be used in the calculations of *CNR* for the system under consideration. These values are chosen or calculated according to the generic ASW mode specification presented in Table 1.

Table 2: Parameters for calculation of clutter to noise ratio for a generic ASW mode.

Parameter	Parameter Value	Effect on CNR
Transmitter power	50000 Watt	46.99 dB
Transmit line losses		-3.29 dB
Antenna gain (two way)		72.00 dB
Antenna ohmic losses	-1.10 dB	
Receiver noise factor	5.00 dB	
Radome loss (two way)		-2.00 dB
Low noise amplifier (LNA) noise figure	1.08 dB	
Temperature of sky	100 K	
Temperature of ground	290 K	
Temperature of array	290 K	
Equivalent noise temperature of antenna	216.26 K	
Equivalent noise temperature of receiver	627.06 K	
Equivalent noise temperature of LNA	23.20 K	
System noise temperature	916.68 K	-29.62 dB
System noise figure	6.19 dB	
Noise Bandwidth	100 MHz	-80.00 dB
SAW device compression gain	250	24.00 dB
SAW device mismatch loss		-2.20 dB

To calculate the mean clutter reflectivity, different sea clutter models can be used [1-4, 29, 30]. Note that for all these models the mean sea clutter reflectivity σ_0 exhibits a number of trends [1-4, 29, 30]:

- The mean clutter reflectivity increases with wind speed (sea state), frequency, and grazing angle,

- The grazing angle dependence is particularly strong at low grazing angles, and

- The mean clutter reflectivity decreases as the look direction moves away from the up-wind direction.

In this report, the mean clutter reflectivity values were calculated using the Georgia Institute of Technology (GIT) sea clutter model [1, 29].

Figure 6 presents the clutter RCS for the analysed ASW mode design in all look directions compared to the wind direction for horizontal polarisation of transmitted and received signals (sea state 3, GIT model). It can be seen that the maximum sea clutter RCS value corresponds to the upwind look direction, the minimum sea clutter RCS value corresponds to the downwind look direction.

Figure 7 presents the *CNR* in all look directions compared to the wind direction for the analysed ASW mode design, the aircraft flying altitude of 1000 ft, and for the wind conditions of sea state 3. It can be seen that, depending on the radar look direction relative to the wind direction, the boundary ranges for the clutter-limited and intermediate detection regions vary: for the chosen ASW mode design for the down-wind look direction the clutter-limited and intermediate region boundary ranges are about 10 n mile and 23 n mile, respectively, and for the up-wind look direction these ranges are about 14 n mile and 27 n mile, respectively.

Therefore, the boundary ranges for detection regions (clutter-limited, intermediate or noise-limited) depend on the flying altitude, the wind speed (sea state) and the radar look direction angles relative to the wind and swell directions. For the same flying altitude, the stronger the wind (i.e. the higher the sea state) and the closer the radar look direction to the up-wind direction, the wider the clutter-limited and intermediate regions. Additionally, if swell is observed, the closer the radar look directions to the up/down swell directions, the wider the clutter-limited and intermediate regions.

3.2.1.4 *Effective Shape Parameter Prediction*

These findings are further confirmed, by Figures 8 and 9 that present the resulting effective shape parameter values[1] of the sea clutter and noise mixture amplitude distribution for the analysed system in all look directions. Figure 8 presents the effective shape parameters in conditions of sea state 3, when swell is not observed. Figure 9 presents the effective shape parameters in conditions of sea state 3, when swell is observed, and the swell direction is the same as the wind direction. The lower the effective shape parameter, the higher the "ideal fixed" threshold that has to be set above the mean clutter and noise mixture level to achieve the desired *Pfa*. Therefore, for the specified false alarm rate, the *Pd* for "ideal fixed" threshold detection is higher at the same detection range for those look directions where the effective shape parameter values are larger.

It means that in the clutter-limited region the problematic detection area may be observed in the following look directions:

- If swell is not observed, in conditions of medium and high sea states – in the up-wind look direction;

- In conditions of the non-equilibrium (developing) medium and high sea states, when the wind and the swell directions are different – in the up-wind, up-swell and down-swell look directions;

- In conditions of a fully developed sea for medium and high sea states – in the up-wind/up-swell and down-wind/down-swell look directions.

---

[1] Note that the maximum value of the effective shape parameter for presentation purposes is taken to be v_{eff} =20 when v_{eff} >20. It is well known that when the K-distribution effective shape parameter is equal to infinity, the K-distribution reduces to the Rayleigh distribution, and for large values (v_{eff} > 20) the sea clutter plus noise amplitude distribution is effectively Rayleigh [1].
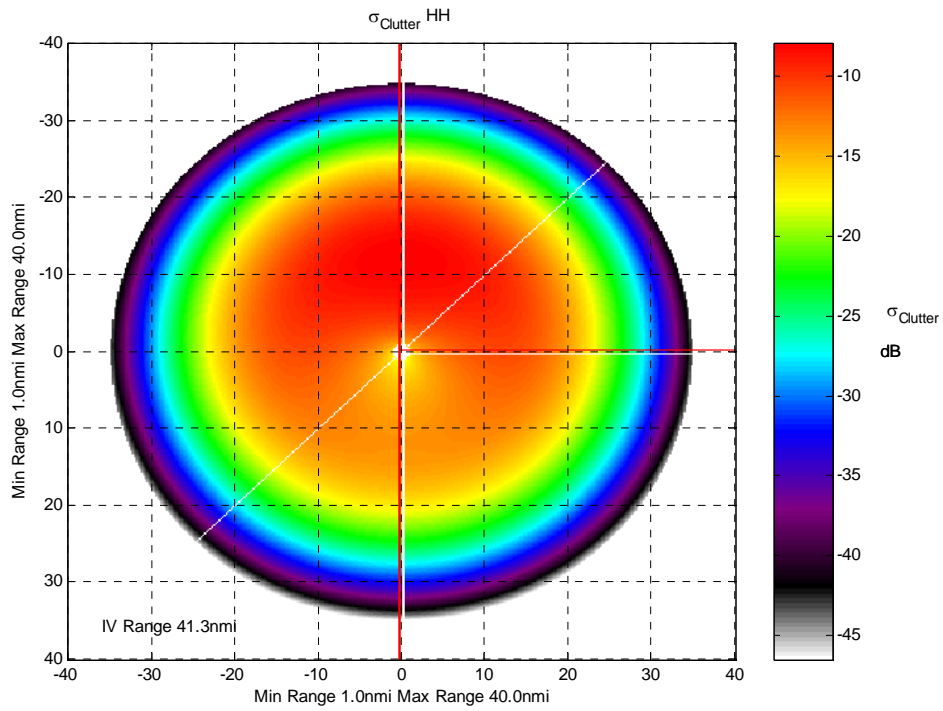
Figure 6: Clutter RCS for the analysed ASW mode design in all look directions compared to the wind direction for a single clutter reflected pulse (sea state 3). The wind is coming from the top of the diagram. Horizontal polarisation.
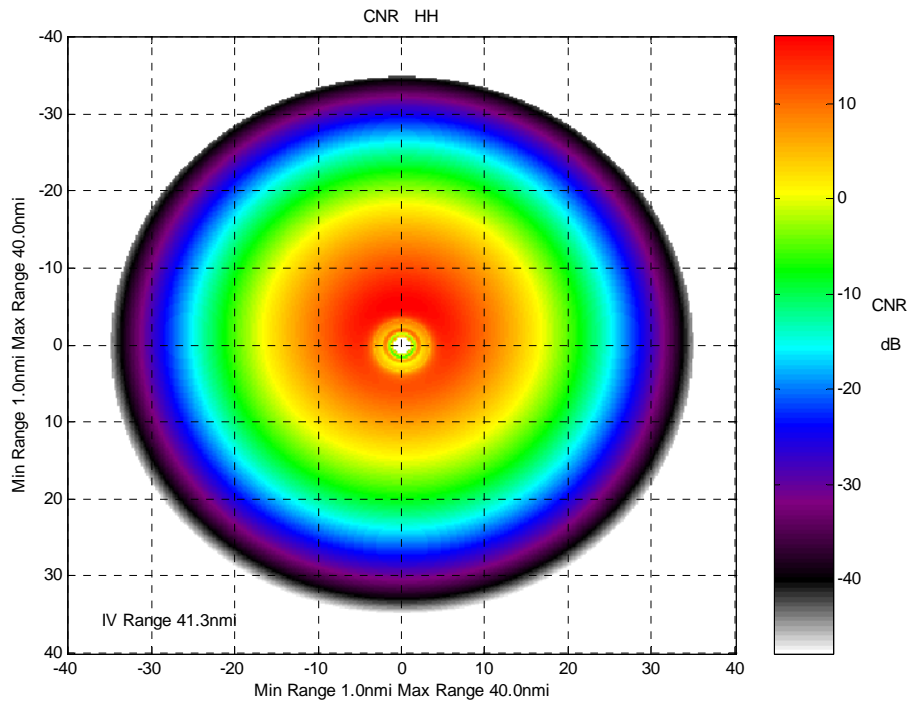
Figure 7: Clutter to noise ratio for the analysed ASW mode design in all look directions compared to the wind direction for a single clutter reflected pulse (sea state 3). The wind is coming from the top of the diagram. Horizontal polarisation.
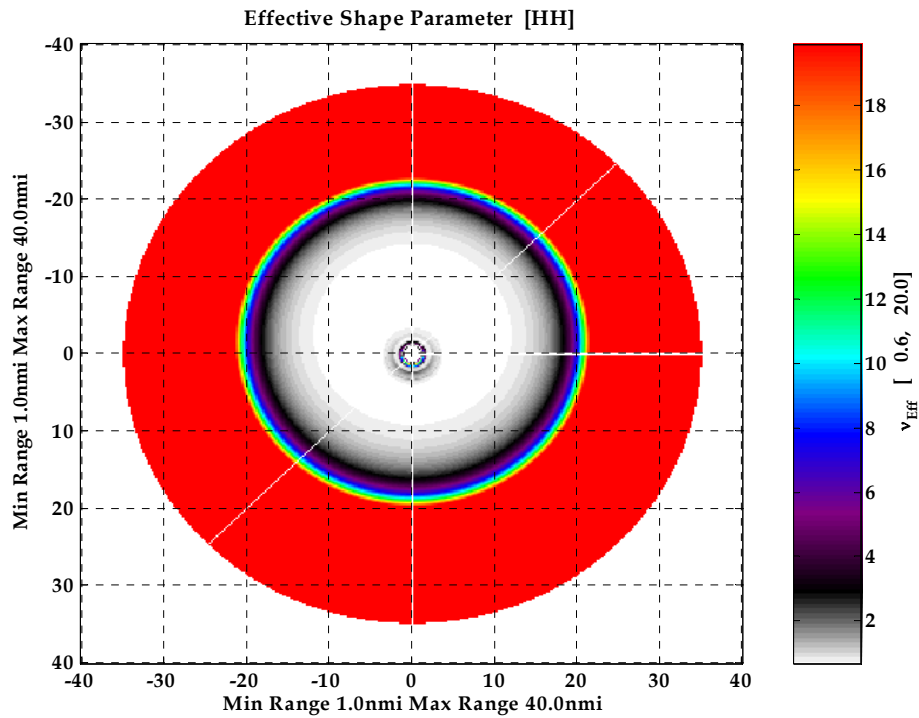
Figure 8: Effective shape parameters in all look directions compared to the wind direction in conditions of a sea state 3, when swell is not observed. The wind is coming from the top of the diagram. Horizontal polarisation.
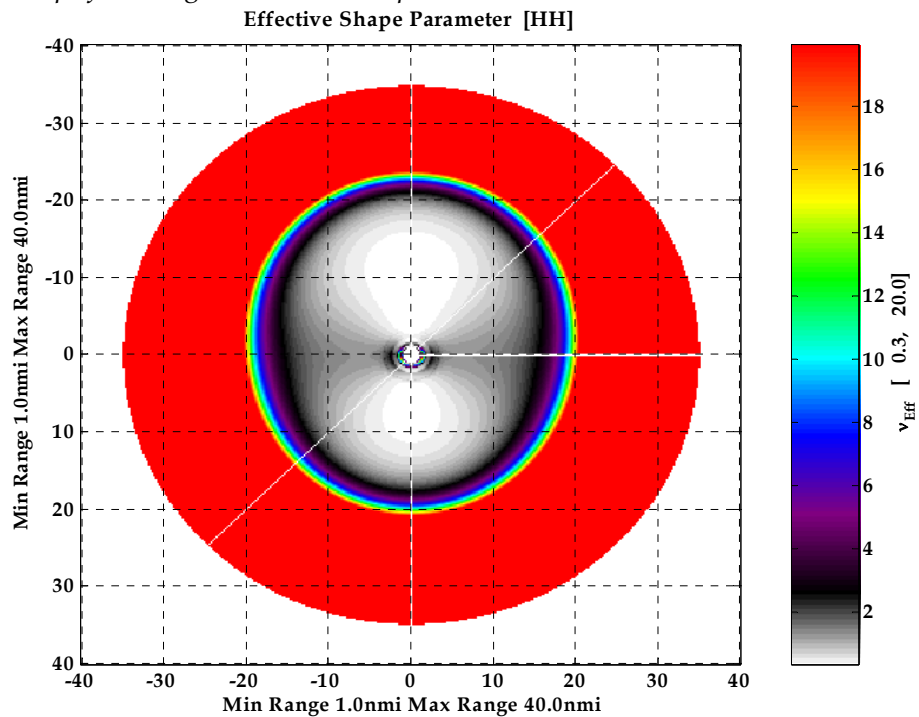
Figure 9: Effective shape parameters in all look directions compared to the swell/wind direction in conditions of a sea state 3, when swell is observed and the swell direction is the same as the wind direction. The wind is coming from the top of the diagram. Horizontal polarisation.

However, recent research results have shown [27, 42 - 48] that in these problematic areas, it may be possible to achieve better detection performance by using "ideal CFAR" threshold detection.

3.2.2 "Ideal CFAR" Threshold Detection

There are potential benefits to be gained by exploiting spatial correlation properties of the clutter.

Spatial correlation of sea clutter reflected signals is a well-known phenomenon [12, 21-24], caused by the modulation of the sea clutter by the surface profile of the sea. While microwave signals are primarily scattered by capillary waves of the sea (speckle), the undulating structure of the sea gravity waves causes variations of the mean power scattered from a given patch (modulating process), which are mechanistically explained in terms of bunching of contributing scatterers and local tilting of the sea surface slope. Thus, it is reasonable to assume that the degree of correlation of the modulating process between resolution cells depends on the spatial correlation of the sea surface, and that this process has a de-correlation distance of the same order of magnitude as the de-correlation distance of the sea.

The correlation length ρ_S of the sea surface in the range direction for a fully developed sea is taken to be a length characteristic of wind waves, given in terms of wind velocity W_V and g, the acceleration due to gravity. It is found that [28]

$$\rho_S = \frac{\pi}{2} \frac{W_V^2}{g} \left(3\cos^2 \theta_W + 1\right)^{1/2}$$

(3.27)

where θ_W is the angle between the line of sight and the wind direction.

If the radar range resolution is ΔR, then the correlation length in radar range samples can be presented as

$$R_{cor} = Tr\left(\rho_S \Big/ \Delta R\right),$$

(3.28)

where $Tr(x)$ rounds x to the nearest integer $\leq x$.

Table 3 presents some values of the correlation length of the sea surface in the range direction, expressed in radar range samples, calculated using (3.28) for a fully developed sea and a given radar range resolution of 0.31 m, when $\theta_W = 0°$ (up-wind look direction) and $\theta_W = 90°$ (cross-wind look direction). It can be seen that for the given radar resolution the correlation length in clutter-limited conditions, expressed in

terms of radar range samples, is large enough for all sea states, if the sea is fully developed[2].

Table 3: Spatial correlation of sea clutter in the up-wind and crosswind look directions in conditions of a fully developed sea.

Sea state	Wind speed W (m/s)	Correlation length, ρ_S (m)		$R_{cor} = Tr\left(\rho_S \middle/ \Delta R \right),\ \ \Delta R = 0.31\,m$	
		$\theta_W = 0°$	$\theta_W = 90°$	$\theta_W = 0°$	$\theta_W = 90°$
1	2.5	2.0	1.0	6	3
2	4.5	6.5	3.2	20	10
3	6.0	11.5	5.8	37	18
4	8.5	23.1	11.6	74	37
5	11.0	38.7	19.4	124	62
6	14.0	62.8	31.4	202	101

Define "ideal detection", for a CFAR processor in K-distributed clutter plus noise mixture, as detection when the noise power and the values of the mean clutter level are exactly known in the two adjacent range patches to the test cell. This assumes that the mean clutter level fluctuation process is first order Markov and that the speckle is independent and identically distributed in adjacent range patches. (If these assumptions are violated, knowledge of the mean clutter level in additional range patches is needed for detection to be "ideal"). In addition, the values of μ, ν and p are assumed to be explicitly known.

For high-resolution sea clutter (at microwaves frequencies) the two components of the compound sea clutter model (Section 3.2), Rayleigh-distributed speckle and Gamma-distributed mean clutter level, represent scattering effects due to small (capillary wave or ripples) and large scale (gravity waves) structures, respectively [21, 25]. For a given realization of the large-scale structure, the small-scale features at two spatially separated patches are uncorrelated and, therefore, their speckle components are modelled by two independent and identically distributed random variables. However, this does not preclude the power backscattered from two spatially separated patches when viewed over the ensemble of large-scale realizations from being correlated. Typically, spatial correlation of scattered power cannot be ignored if the physical separation of the patches is less than the correlation length of large-scale structures. This effect is taken into account by modelling the mean intensity of the clutter $u_i = 4y_i^2/\pi$ and $u_k = 4y_k^2/\pi$ reflected from two spatially separated patches as correlated random variables with the correlation coefficient determined as

---

[2] Note that if sea is not fully developed, in the presence of swell the correlation length ρ_S of the sea surface in the range direction has to be replaced by half the swell wavelength for the up and down swell look directions. Looking across the swell direction breaks up the swell pattern.

$$p_{ik} = \frac{E\{[u_i - E(u_i)][u_k - E(u_k)]\}}{\sigma_u^2} = \frac{E(u_i u_k) - E^2(u_i)}{\sigma_u^2}, \tag{3.29}$$

where i and k denote the spatial position of the patches and $E\{x\}$ is the expectation operator. The two random variables u_i and u_k are assumed to have the same variance σ_u^2.

The joint PDF of the correlated Gamma-distributed random variables, u_i and u_k, is given by [21, 22, 23, 40]

$$p(u_i, u_k) = p(u_i) p(u_k) \frac{\Gamma(\nu)}{(1 - p_{ik})} \left[\frac{u_i u_k p_{ik}}{b^4} \right]^{-\frac{\nu-1}{2}} \exp\left[-\frac{p_{ik}}{1 - p_{ik}} \frac{(u_i + u_k)}{b^2} \right] I_{\nu-1}\left[\frac{2\sqrt{u_i u_k p_{ik}}}{b^2(1 - p_{ik})} \right] \tag{3.30}$$

where

$$p(u) = \frac{b^{2\nu}}{\Gamma(\nu)} u^{\nu-1} \exp(-b^2 u). \tag{3.31}$$

The joint PDF of the correlated Chi-distributed random variables, y_i and y_k, is given by [21, 22, 23, 40]

$$p(y_i, y_k) = p(y_i) p(y_k) \frac{\Gamma(\nu)}{p_{ik}^{\frac{o-1}{2}}(1 - p_{ik})} \left[\frac{y_i y_k}{b^4} \right]^{-\nu} \exp\left[-\frac{p_{ik}}{1 - p_{ik}} \frac{(y_i^2 + y_k^2)}{b^2} \right] I_{\nu-1}\left[\frac{2\sqrt{y_i^2 y_k^2 p_{ik}}}{b^2(1 - p_{ik})} \right] \tag{3.32}$$

where $p(y) = \frac{2 b^{2\nu}}{\Gamma(\nu)} y^{2\nu-1} \exp(-b^2 y^2)$.

Then, the conditional PDF of the mean clutter intensity u is given by

$$p(u_i/u_k) = \frac{p(u_i, u_k)}{p(u_k)}$$

$$= \frac{1}{b^2(1 - p_{ik}) p_{ik}^{\frac{\nu-1}{2}}} \left(\frac{u_i}{u_k} \right)^{\frac{\nu-1}{2}} \exp\left[-\frac{u_i + p_{ik} u_k}{b^2(1 - p_{ik})} \right] I_{\nu-1}\left[\frac{2\sqrt{u_i u_k p_{ik}}}{b^2(1 - p_{ik})} \right] \tag{3.33}$$

The conditional PDF of the mean clutter amplitude level y is obtained as

$$p(y_i/y_k) = \frac{1}{b^2(1-p_{ik})p_{ik}^{\frac{\nu-1}{2}}} \left(\frac{y_i}{y_k}\right)^{(\nu-1)} \exp\left[-\frac{y_i^2 + p_{ik}y_k^2}{b^2(1-p_{ik})}\right] I_{\nu-1}\left[\frac{2\sqrt{y_i^2\,y_k^2\,p_{ik}}}{b^2(1-p_{ik})}\right] \quad (3.34)$$

If the random variables u_i and u_k representing the clutter samples are a first-order Markov process, then for the mean clutter intensities with exponential autocorrelation functions (ACFs) we have

$$p(u_i...u_n) = p(u_1/u_2)\,p(u_2/u_3)...p(u_{n-1}/u_n)\,p(u_n) \qquad (3.35)$$

$$p(y_i...y_n) = p(y_1/y_2)\,p(y_2/y_3)...p(y_{n-1}/y_n)\,p(y_n) \qquad (3.36)$$

and the correlation coefficient between the mean clutter levels in i-th and j-th range cells can be expressed as

$$p_{ij} = p^{|i-j|}, \qquad 0 < p < 1, \qquad (3.37)$$

where p is the correlation coefficient between adjacently received clutter samples, which can be determined for a fully developed sea in the clutter-limited region by using the correlation length of the sea surface in the range direction, expressed in radar range samples (3.28)

$$p \approx 0.1^{\frac{1}{R_{cor}}} \qquad (3.38)$$

The join PDF of the overall clutter plus noise amplitudes w_i and w_k can be obtained by taking into account the respective speckle components and hence from (3.10) and (3.32)

$$p(w_i, w_k) = \int_0^\infty \int_0^\infty p(w_i/y_i)\,p(w_k/y_k)\,p(y_i, y_k)\,dy_i\,dy_k \qquad (3.39)$$

Then, the detection threshold is determined only by the known values of the noise power and the mean clutter level in the two adjacent range patches to the test cell, y_E and y_L. The expected value of the false alarm probability is given by

$$\left(\overline{P}_{fa}\right)_{ideal} = \int_0^\infty \left[\int_0^\infty\int_0^\infty \exp\left(-\frac{t_{ideal}}{2\sigma^2 + 4y_0^2/\pi}\right) p(y_E, y_L)\,dy_E dy_L\right] p(y_0/y_E, y_L)\,dy_0$$

$$= \int_0^\infty\int_0^\infty \exp\left(-\frac{\beta_{ideal}\,\overline{z}}{\mu\left(1 + \dfrac{1}{CNR}\right)}\right) p(y_E, y_L)\,dy_E\,dy_L, \qquad (3.40)$$

The P_d for "ideal detection" for a Swerling 2 target is given by

$$\left(\overline{P}_d\right)_{ideal} = \int\limits_0^\infty \int\limits_0^\infty \int\limits_0^\infty \exp\left(-\frac{t_{ideal}}{2\sigma^2+4y_0^2/\pi+\overline{A}^2}\right) p\left(y_0/y_E,y_L\right) p\left(y_E,y_L\right) dy_0\, dy_E\, dy_L$$

$$= \int\limits_0^\infty \int\limits_0^\infty \exp\left(-\frac{\beta_{ideal}\,\overline{z}}{\mu\left(1+\dfrac{1}{CNR}\right)(1+S(C+N)R)}\right) p\left(y_E,y_L\right) dy_E\, dy_L \qquad (3.41)$$

Figure 10 presents the dependencies of expected ideal detection losses in spiky K-distributed sea clutter compared to the Rayleigh clutter plus noise mixture on the effective shape parameter of clutter plus noise amplitude distribution and correlation properties for given $Pfa = 10^{-6}$ and $Pd = 0.5$ [23].
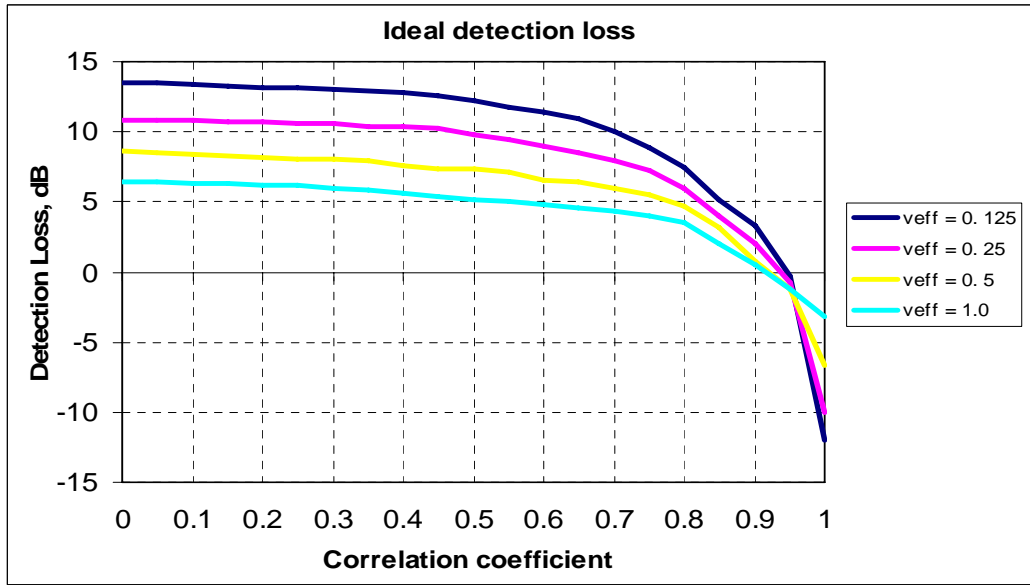
Figure 10: Ideal detection loss in spatially correlated K-distributed clutter plus noise mixture compared to detection in Rayleigh clutter plus noise mixture for Pfa = 10^{-6} and Pd = 0.5.

Here the detection loss for $p = 0$ represents the case of "ideal fixed" threshold detection, which is optimal if K-distributed sea clutter plus noise mixture is spatially uncorrelated. The results for $p = 1$ corresponds to the case of "ideal CFAR" detection, when the mean clutter plus noise level in the test cell is known exactly.

It is evident that, CFAR processing in the clutter-limited detection region with a short cell-averaging length for moderate to high values of p in order to follow slow variations of the mean clutter plus noise level, it is possible to achieve several dBs of the detection gain relative to the case of CFAR processing with a long cell-averaging length that produces the results close to those for the "ideal fixed" threshold detection.

The conventional approach to estimate detection losses of the threshold setting for any radar system is to compare it with an "ideal fixed" threshold. Then, the maximum possible values of CFAR gain (i.e. the minimum negative CFAR loss values) are given by the difference between the "ideal fixed" and "ideal CFAR" thresholds.

Theoretically if the "ideal CFAR" conditions were to be achieved, the value of the threshold-multiplying factor β required would be independent of the distribution of the clutter local mean level.

Thus, for "ideal CFAR" threshold detection in K-distributed strong sea clutter, when the local clutter level y is known explicitly and noise can be neglected, the appropriate value of the threshold multiplier $\beta_{ideal\ CFAR}$ is determined using the relationship [27, 42]

$$ t = \beta_{ideal\ CFAR}\ \mu = -\frac{4y^2}{\pi} \log_e\left(\overline{P}_{fa}\right) \tag{3.42} $$

The overall P_d for "ideal CFAR" threshold detection of a Swerling 2 target in K-distributed sea clutter is given by

$$ \left(\overline{P}_d\right)_{ideal\ CFAR} = \int_0^\infty \frac{2b^{2\nu}}{\Gamma(\nu)}\ y^{2\nu-1}\ \exp\left(-b^2 y^2\right) \exp\left(-\frac{\beta_{ideal\ CFAR}\ \mu}{4y^2/\pi + \overline{A}^2}\right) dy \tag{3.43} $$

For "ideal CFAR" threshold detection in sea clutter combined with non-negligible noise, when the local clutter plus noise level y and σ^2 are known explicitly, the appropriate value of the threshold multiplier $\beta_{ideal\ CFAR}$ will be fixed at that required for the speckle component of the clutter (i.e. Gaussian clutter, with the shape parameter $\nu = \infty$) and noise

$$ t = \beta_{ideal\ CFAR}\ \mu = -\left(2\sigma^2 + \frac{4y^2}{\pi}\right) \log_e\left(\overline{P}_{fa}\right) \tag{3.44} $$

The overall P_d for "ideal CFAR" threshold detection of a Swerling 2 target in K-distributed clutter combined with noise is determined as

$$ \left(\overline{P}_d\right)_{ideal\ CFAR} = \int_0^\infty \frac{2b^{2\nu}}{\Gamma(\nu)}\ y^{2\nu-1}\ \exp\left(-b^2 y^2\right) \exp\left(-\frac{\beta_{ideal\ CFAR}\ \overline{z}}{2\sigma^2 + 4y^2/\pi + \overline{A}^2}\right) dy\ . \tag{3.45} $$

3.2.3 Comparison of "Ideal Fixed" and "Ideal CFAR" Threshold Detections

To demonstrate the differences in the expected performance of the "ideal fixed" and "ideal CFAR" threshold detectors for the same conditions, as an example, Figure 11 shows the values of the threshold multiplier β (i.e. $S(C+N)R$) required to achieve $\overline{P}_d = 0.5$ for "ideal fixed" and "ideal CFAR" detection as a function of the K-distribution shape parameter ν and the CNR when the $\overline{P}_{fa}$ is set to 10^{-4}. From

Figure 11, it can be seen that the "ideal CFAR" detection performance, which is presented by dashed lines, is more sensitive to the presence of thermal noise, approaching more rapidly the detection performance expected in noise alone as the *CNR* falls. For "ideal fixed" threshold detection, which is presented by solid lines, the performance in spiky sea clutter (i.e. low values of ν) is determined to a large extent by the clutter spikes even in relatively low *CNR*s [27, 42].
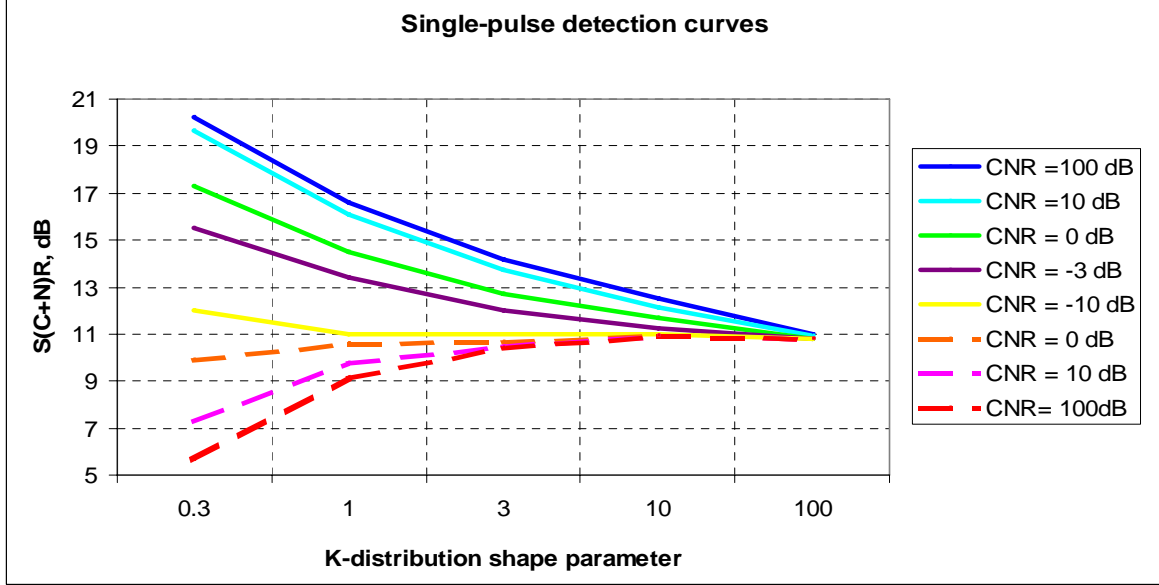
Figure 11: Single-pulse detection curves for a Swerling 2 target in clutter and noise for various values of CNR, $\overline{P}_d = 0.5$ and $\overline{P}_{fa} = 10^{-4}$ (solid lines – "ideal fixed" threshold, dashed lines – "ideal CFAR" threshold).

In practice, the "ideal CFAR" case, which is able to follow the mean level variations of clutter, will not be achieved, but considerable better performance (i.e. "CFAR gain") than an "ideal fixed" threshold may be achievable. In some cases, such as very spiky and/or spatially uncorrelated clutter, or weak compared to noise clutter, it may be impossible to follow the clutter mean level variations. Under those circumstances "ideal fixed" threshold detection performance represents the best that can be achieved. Therefore, in order to predict the best detection performance that a high-resolution maritime radar system with the specified parameters can achieve in certain conditions, it is important to understand whether the "ideal fixed" or "ideal CFAR" threshold detection setting is optimal in these conditions.

The analysis of "ideal" detection performance in Sections 3.2.1 and 3.2.2 was done under the assumption that the PDF of clutter amplitude (i.e. the mean level and shape parameter) and *CNR* are known explicitly. In practice, however, these parameters are not known a priori and need to be estimated.

Different types of CFAR processor can be used to estimate the mean level of clutter plus noise mixture $\overline{z}$, the effective clutter plus noise amplitude distribution shape parameter ν_{eff} and *CNR*. In any CFAR processor, the appropriate value of threshold

multiplier β is chosen to achieve the desired value of probability of false alarm in the absence of a target. However, the value of β is dependent not only on the PDF of clutter amplitude and the *CNR*, as it is for the "ideal fixed" and "ideal CFAR" threshold detectors, but on characteristics of the cell-averaging filter and the algorithm used to estimate the effective shape parameter of the clutter plus noise amplitude distribution [13, 14, 24].

3.3 Nature of CFAR Loss in Basic Design CFAR Processors

Assume that the clutter returns for any particular surveillance area are given by a sequence of K-distributed samples x_{ji} (*i* = 0, …, *N* - *1*) having mean level y_j. Samples of the mixture of these K-distributed signals and noise, w_{ji}, which are used for estimation of the mean clutter plus noise level of the cell under test, are locally Rayleigh distributed variates with a fixed mean level value $\sqrt{\dfrac{\pi}{2}\sigma^2 + y_j^2}$.

Note that for pulse repetition intervals encountered in an airborne maritime surveillance radar, independent samples of the overall clutter amplitude K-distribution are never obtained from pulse to pulse in sea clutter, except for the limiting case of Rayleigh distributed clutter.

Further analysis of a generic ASW mode detection performance is based on two major assumptions that follow from the signal processing technique applied, the compound nature of the sea clutter and relationships between the temporal radar system parameters and the sea clutter temporal correlation function:

1. The radar integration time is short compared to the correlation period of the underlying mean level component of the sea clutter, so that this mean level can be considered as constant (fully correlated from pulse to pulse) during the integration time. This is a feasible assumption as the correlation period of the underlying level component is an order of a few seconds while the integration time is a few milliseconds.

2. Independent samples of the speckle component are achieved by the use of frequency agility. During the integration period (with mean clutter level being constant) amplitude samples of the sea clutter return are independent Rayleigh distributed variates.

The radar CFAR processor is required to adapt its processing to match the clutter environment as it changes with range and look direction.

As discussed in Section 3.2.1.3, the mean clutter plus noise level changes with change in range and look direction over the area of operation of the radar quite widely. Therefore, the radar needs to adapt to the changing clutter plus noise amplitude levels in order to maintain CFAR from area to area.

Sections 3.2.1 and 3.2.2 show that for K-distributed sea clutter, the optimal threshold-multiplying factor value β is determined by the effective shape parameter of the amplitude distribution of the clutter and noise mixture and the clutter and noise mixture correlation properties. As the values of the clutter shape parameter and the CNR vary over the area of operation of the radar quite widely (see Sections 3.2.1.2 and 3.2.1.3 of the report), the threshold-multiplying factor β ≅must be changed accordingly in order to maintain CFAR from area to area. Therefore, the adaptation of this multiplying factor β to changes in the effective shape parameter of the amplitude distribution of the clutter and noise mixture is just as important as the need to adapt to the changing clutter plus noise amplitude levels.

From Section 3.2.2 of the report, it is also clear that a practical radar must be able to adapt its cell-averaging length according to the changes in the correlation properties of the clutter plus noise mixture, if the best performance is to be achieved [13, 38, 39].

Figure 12 presents a basic configuration for a typical CFAR processor. Note that it is usually assumed that distributions of the threshold and the cell under test are independent for all CFAR processors under consideration. This is achieved by leaving a gap, *G*, between the cell under test and the nearest range samples used in the cell-averaging filter, to allow for the over-sampling in range of the data which occurs in practice [24].
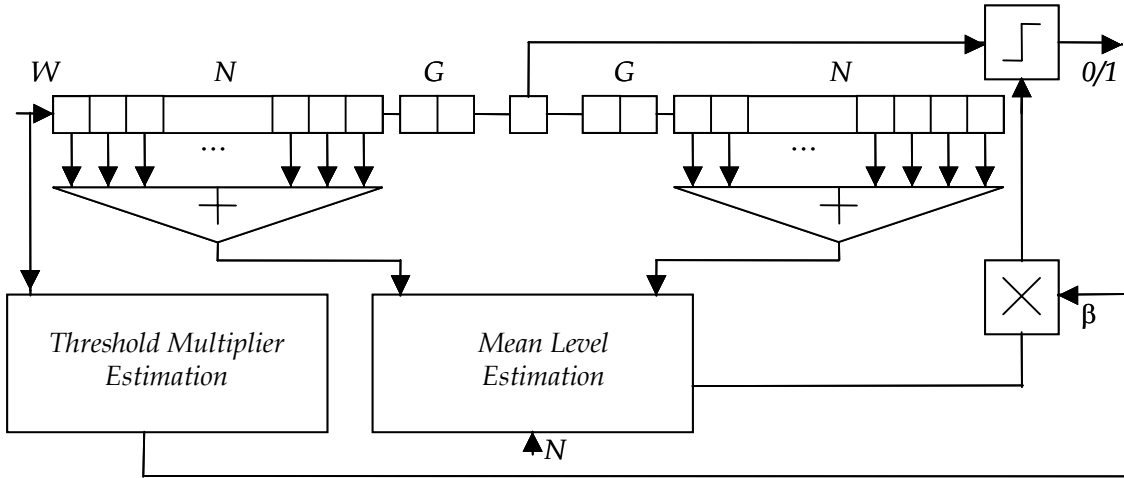
Figure 12: Basic CFAR processor configuration. CFAR length 2N; CFAR gap = G.

For successive radar return *W*, sampled in range, the estimate of mean level $\hat{z}_j$ given by any type of cell-averaging filter will be in error, due to the finite sample size, *2N*. The threshold $t = \beta \hat{z}_j$ will fluctuate in time resulting in a higher required value of β compared to the "ideal" threshold case to achieve a given value of probability of false alarm.

In case of the cell-averaging filter with a large number of reference cells *N* used in the detection process, the threshold setting for any CFAR area is determined by the overall parameters of the amplitude distribution of clutter plus noise mixture for the test area.

If the shape parameter of the sea clutter distribution and the *CNR* can be estimated as they vary over the area of operation of the radar, then the appropriate value of the threshold-multiplying factor β could be calculated for a given "global" mean clutter plus noise level [8, 26, 27]. Thus, the CFAR processor with a large number of reference cells should have the detection performance that is close to the "ideal fixed" threshold detector.

In case of the cell-averaging filter with a small number of reference cells used in the detection process, the threshold setting is based on the clutter plus noise "local" mean level estimation. Theoretically if the "ideal CFAR" conditions were to be achieved, the value of the threshold-multiplying factor, β, required would be independent of the distribution of the clutter plus noise local mean level. In practice, some control of β is still required, but the range of values expected over a clutter-limited region of radar search area may be considerably reduced [13, 24].

In both cases, errors in setting the appropriate value of the threshold multiplier resulting in a higher required value of β compared to the "ideal" threshold case.

Therefore, the estimation of the mean clutter plus noise level in the cell under test $\hat{z}_j$ and the threshold-multiplying factor β is subject to random errors that force the use of the threshold multiplier values higher than would be used if the estimate were exact. If the differences between the true and the estimated values of these parameters are not allowed for, then the threshold can be set too low and the false alarm rate will be too high. In particular, such a situation is possible when the mean clutter plus noise level is underestimated and/or the clutter shape parameter is overestimated.

The estimated threshold-multiplying factor $\hat{\beta}$ (dB) is related to the ideal by

$$\hat{\beta} = \beta_{ideal} + \beta_{MEAN} + \beta_{THR} \tag{3.46}$$

where β_{MEAN} is the error of the mean level estimation and β_{THR} is the error of the threshold multiplier estimation, related to the errors of the shape parameter and the *CNR* estimation.

Note that the increase in the threshold-multiplying factor β to achieve a given average false alarm rate, above that required if clutter plus noise mixture parameters had been estimated exactly, corresponds to the reduction in the achievable *Pd* for a given *S(C+N)R*.

Then, the CFAR loss, L_{CFAR}, can be determined as the additional *S(C+N)R* required to achieve *Pd* with given *Pfa*, over and above that for "ideal fixed" threshold detection in mixture of K-distributed clutter and noise.

According to (3.19) the value of CFAR loss (dB) is given as

$$L_{CFAR} \;\; = \;\; L_{MEAN} + L_{THR} \tag{3.47}$$

The CFAR loss of the mean clutter plus noise level estimation, as measured by the change in *S(C+N)R* required to maintain *Pd* for a given *Pfa* , differs according to the type of CFAR processor used and will be a function of a target type, *Pfa* and *Pd*, as well as spatial correlation properties of clutter plus noise mixture, a *CNR* and a shape parameter of the clutter plus noise amplitude distribution. For a given CFAR design, the CFAR loss value of the mean clutter plus noise level estimation is different for different statistical properties of clutter plus noise mixture. In particular, the optimal number of reference cells the CFAR processor should use for the mean clutter plus noise estimation is determined by the spatial correlation properties of clutter and noise mixture and *CNR*.

Hence, it is necessary to consider the CFAR loss of the mean clutter plus noise level estimation for the following cases:

1. When clutter plus noise mixture is spatially uncorrelated and Rayleigh-distributed (Section 3.5.1). For any type of a CFAR detector, in Rayleigh clutter plus noise mixture the CFAR loss of the mean level estimation is a function of *Pfa*, *Pd*, a target model, the cell-averaging length and the number of pulses integrated prior to CFAR processing.

2. When clutter plus noise mixture is spatially uncorrelated or weakly correlated, and has a non-Rayleigh distribution (Section 3.5.2.1). In spatially uncorrelated non-Rayleigh clutter plus noise mixture, the CFAR loss of the mean level estimation is additionally a function of the shape parameter and *CNR*.

3. When clutter plus noise mixture is strongly spatially correlated and non-Rayleigh-distributed (Section 3.5.2.2). In spatially correlated non-Rayleigh clutter plus noise mixture, the interaction between the cell-averaging CFAR and the clutter theoretically can produce a CFAR gain. The highest values of CFAR gain are achieved with a short cell-averager length in highly spatially correlated clutter. However, such short cell-averagers will also produce the highest CFAR loss in uncorrelated clutter or noise-limited conditions.

The following sections of the report present the analytical results for numerical estimation of the values of CFAR loss for each of the above cases for three basic design CFAR processors that use:

- Either the "cell-averaging", or "greatest of", or "smallest of" logic for the estimation of the mean level of the sea clutter plus noise amplitude distribution, and

- A number of different algorithms for the estimation of this distribution variance (represented by the shape parameter).

3.4   CFAR loss of the Mean Clutter Plus Noise Level Estimation

Consider the value of CFAR loss of the mean clutter plus noise level estimation for a typical radar system CFAR processing design on an example of three basic CFAR filter configurations that are commonly used in practice [2-4, 6-8, 17]:

- "Cell-averaging" (CA) CFAR processor, presented in Figure 13,

- "Greatest of" (GO) CFAR processor, presented in Figure 14, and

- "Smallest of" (SO) CFAR processor, presented in Figure 15.
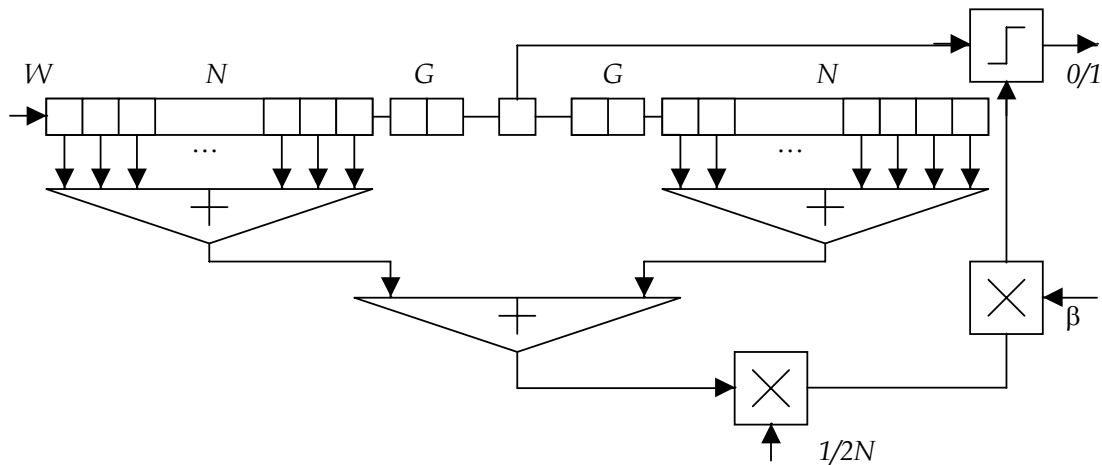
Figure 13: "Cell-averaging" CFAR processor. CFAR length 2N; CFAR gap = G.
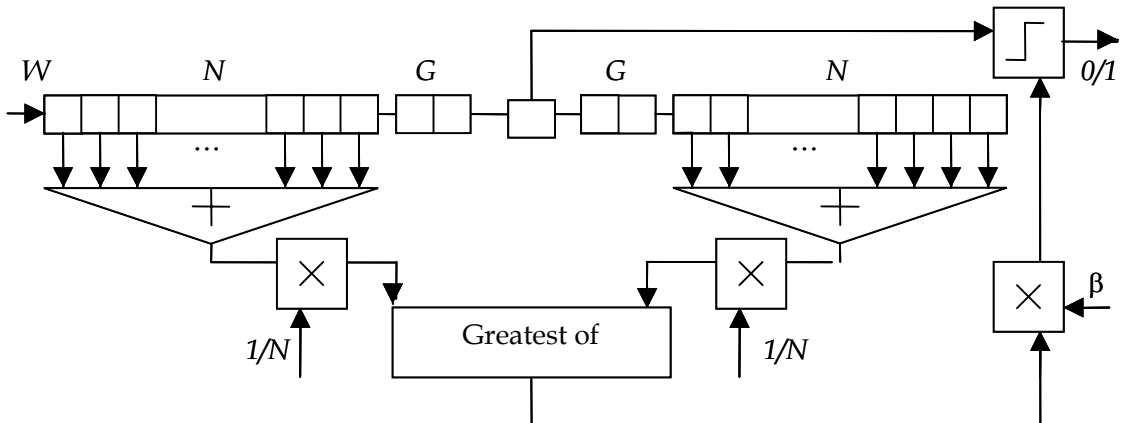
Figure 14: "Greatest of" CFAR processor. CFAR length 2N; CFAR gap = G.
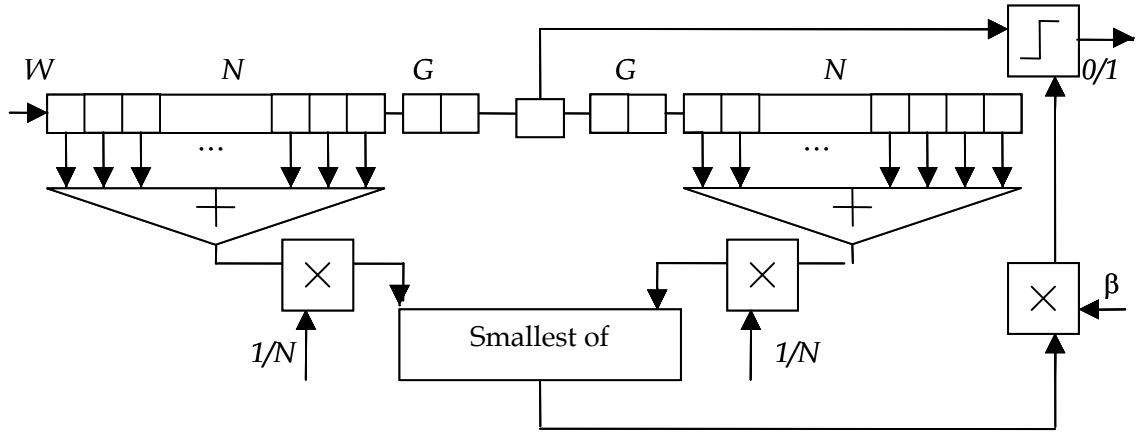
Figure 15: "Smallest of" CFAR processor. CFAR length 2N; CFAR gap = G.

For a CA CFAR processor, the running average is performed over *2N* range samples of double-sided reference windows (Figure 13), where *N* is the number of range samples that are averaged from each side of the cell under test.

The threshold for the CA CFAR processor at a given instant is derived based on estimated values of the mean clutter plus noise level z_j for the cell under test and multiplying factor $\hat{\beta}$

$$t_{CA} = \hat{\beta} * \frac{1}{2N} \sum_{i=1}^{2N} w_{ji} = \hat{\beta} * \hat{z}_{CAj}, \tag{3.48}$$

where:

w_{ji} *(i = 1, …, 2N)* are the overall K-distributed clutter and noise mixture random variates;

$\hat{\beta}$ is a multiplying factor, chosen to give the required *Pfa*;

$\hat{z}_{CAj}$ is the mean clutter plus noise level estimate for *j* cell under test; and

2N is a number of samples used for the mean clutter plus noise level estimation.

For a given number of reference cells this provides minimum loss under conditions of homogeneous Rayleigh noise background. If the noise in the reference cells is corrupted by the presence of additional targets or large discrete clutter sources (extraneous targets), or if the CFAR window covers transitions from one clutter power to another, then an increase in the *Pfa* and a reduction in the detection probability *Pd* (target masking) can result [2-4, 6-8, 17].

A GO CFAR processor (Figure 14) was introduced to counter the problem of transitions in clutter power (clutter edges). For the GO CFAR the running averages are performed separately in each window that consists of *N* range samples taken from

each side of the cell under test and then these averages compared to choose the "greatest of" value.

The threshold for the GO CFAR processor at a given instant is derived based on the estimated values of the "greatest of" selection between the leading and lagging sets of reference cells (corresponding mean clutter plus noise levels) of the cell under test and multiplying factor $\hat{\beta}$

$$ t_{GO} \;=\; \hat{\beta} * \max\left[\frac{1}{N}\sum_{i=1}^{N} w_{ji}, \;\; \frac{1}{N}\sum_{i=N+1}^{2N} w_{ji}, \right] \;=\; \hat{\beta} * \hat{z}_{GOj}, \tag{3.49} $$

where:

$\hat{\beta}$ is a multiplying factor, chosen to give the required *Pfa*;

$\hat{z}_{GOj}$ is the "greatest of" selection between the leading and lagging mean clutter plus noise level estimates for the cell, j, under test; and

N is a number of samples used for each mean clutter plus noise level estimation.

This results in better performance in non-homogeneous clutter at the expense of slightly increased loss than the CA CFAR processor. The GO CFAR processor is extremely sensitive to extraneous targets [6-8, 17].

A SO CFAR processor (Figure 15) was proposed as a means of overcoming the problem of extraneous targets. For the SO CFAR the running averages are performed separately in each window that consists of N range samples taken from each side of the cell under test and then these averages are compared to choose the "smallest of" value.

The threshold for the SO CFAR processor at a given instant is derived based on the estimated values of the "smallest of" selection between the leading and lagging sets of reference cells (corresponding mean clutter plus noise levels) of the cell under test and multiplying factor $\hat{\beta}$

$$ t_{SO} \;=\; \hat{\beta} * \min\left[\frac{1}{N}\sum_{i=1}^{N} w_{ji}, \;\; \frac{1}{N}\sum_{i=N+1}^{2N} w_{ji}, \right] \;=\; \hat{\beta} * \hat{z}_{SOj} \tag{3.50} $$

where

$\hat{\beta}$ is a multiplying factor, chosen to give the required *Pfa*;

$\hat{z}_{SOj}$ is the "smallest of" selection between the leading and lagging mean clutter plus noise level estimates for cell , j, under test; and

N is a number of samples used for each mean clutter plus noise level estimation.

This gives improved performance in the presence of extraneous targets.

3.4.1 CFAR Loss of the Mean Level Estimation in Spatially Uncorrelated Rayleigh Clutter Plus Noise Mixture

The Rayleigh amplitude characteristics of spatially uncorrelated clutter plus noise mixture for a generic ASW mode design are observed in the noise-limited region of the ASW mode detection performance.

For the specified values of *Pd*, *Pfa* and the number of independent averaged cells *2N*, the CFAR loss of mean level estimation for two basic CFAR detectors of the analysed radar system ASW mode design, CA CFAR and GO CFAR, with different detection laws in Rayleigh clutter plus noise mixture can be determined using the universal CFAR loss curve [2] presented in Figure 16.
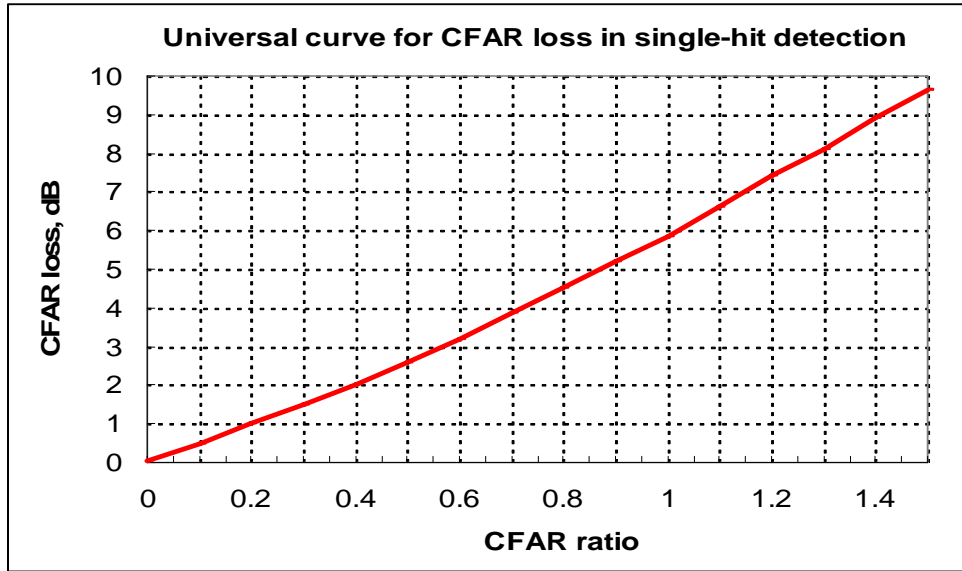
Figure 16: Universal curve for CFAR loss of the mean level estimation in single-hit detection, for a steady or fluctuating target.

This curve presents CFAR loss as a function of the CFAR ratio $n/(2N_{eff})$, where $n = -\log_{10}(\overline{P}_{fa})$ and *2Neff* is the effective number of reference samples in single-hit detection in Rayleigh clutter/noise, for $Pd \geq 0.9$.

To determine the CFAR loss for Pd =0.5, it is necessary to subtract $8/(2N_{eff})$ % from the dB-value of CFAR loss determined for $Pd \geq 0.9$ [2].

Note that if the number of reference cells is large enough, the influence of varying *Pd* in the range $0.3 \leq Pd \leq 0.9$ is practically negligible and can be omitted from the analysis [5, 14].

The effective number of reference cells, *2N$_{eff}$*, is calculated as follows

$$2N_{eff} \;=\; \frac{(2N+k)}{1+k}, \tag{3.51}$$

where values of k are shown in Table 4.

Table 4: Constants determining number of effective CFAR reference samples.

CFAR detector type	k
Square-law detector	1
Linear envelope detector	0.09
Greatest-of CFAR, square-law detector	0.37
Greatest-of CFAR, linear envelope detector	0.5

To illustrate how the corresponding CFAR loss of the mean clutter plus noise level estimation can be determined analytically, consider in the following sections of the report the results for the three considered basic CFAR detectors (CA, GO and SO) in Rayleigh clutter plus noise mixture for a Swerling 2 target model and square law detector.

3.4.1.1 CFAR Loss of the Mean Level Estimation in Rayleigh Clutter Plus Noise Mixture for a CA CFAR Square-law Detector

For a square law detector, the PDF of Rayleigh-distributed clutter plus noise mixture following the integration of M pulses is given by [13]

$$p(w) \;=\; \frac{1}{\bar{z}_{CA}^M}\,\frac{w^{M-1}}{\Gamma(M)}\,\exp\!\left(-\frac{w}{\bar{z}_{CA}}\right), \qquad \left(0 \le w \le \infty\right) \tag{3.52}$$

If the cell-averager uses $2N$ samples, then the CFAR threshold, t_{CA}, will have a distribution given by:

$$p(t_{CA}) \;=\; \frac{1}{\bar{z}_{CA}^{2NM}}\left(\frac{2N}{\beta}\right)^{2NM}\frac{t_{CA}^{2NM-1}}{\Gamma(2NM)}\,\exp\!\left(-\frac{2N\,t_{CA}}{\beta\,\bar{z}_{CA}}\right), \qquad \left(0 \le t_{CA} \le \infty\right) \tag{3.53}$$

The *Pfa* following this threshold is given by (3.54), where $_2F_1$ is a hypergeometric function

$$\begin{aligned}
P_{fa} \;&=\; \int\limits_0^\infty \left(\int\limits_t^\infty p(w)\,dw\right) p(t_{CA})\,dt_{CA} \\[2mm]
&=\; \left(\frac{2N}{\beta}\right)^{2NM}\frac{\Gamma(M+2NM)}{\Gamma(M)\,\Gamma(2NM+1)}\; _2F_1\!\left[2NM,\,M+2NM;\,-2N/\beta\right]
\end{aligned} \tag{3.54}$$

The value of β required to give a desired value of *Pfa* in equation (3.54) can then be compared with the "ideal fixed" threshold, given by

$$\left(P_{fa} \right)_{ideal\ fixed} \;=\; \frac{\gamma(M,\ \beta_{ideal\ fixed}\ M)}{\Gamma(M)} \tag{3.55}$$

where $\gamma(b,\ a) \;=\; \displaystyle\int_0^a \frac{x^{b-1}}{\Gamma(b)}\,\exp(-x)\,dx$ is the incomplete Gamma function.

It can be seen that the increase in β compared to β *ideal fixed* depends on the number of reference cells *2N* and the number of non-coherently averaged pulses *M* prior to CFAR processing.

As there is no non-coherent integration of single pulse returns prior to CFAR processing in the chosen ASW mode design, we are primarily interested in the case of CFAR detection of single pulse returns.

Thus, for CFAR threshold detection of single pulse returns (*M* =1), the *Pfa* is given by

$$P_{fa} \;=\; \left[1 + \frac{\beta}{2N} \right]^{-2N}, \tag{3.56}$$

and the *Pfa* for "ideal fixed" threshold detection is determined by:

$$\left(P_{fa} \right)_{ideal\ fixed} = \exp\!\left(-\beta_{ideal\ fixed} \right) \tag{3.57}$$

To determine the CFAR loss value for CFAR threshold detection of single pulse returns, consider the probabilities of detection achieved in the CA CFAR and "ideal fixed" threshold detectors.

For single pulse detection of a target with a Swerling 2 characteristics and a given *S(C+N)R* at the input of the square-law detection, the PDF of the signal plus clutter plus noise sample is

$$p_{W+S}(w) \;=\; \frac{1}{z_{CA}\left[1 + S(C+N)R\right]}\,\exp\!\left\{ -\frac{w}{z_{CA}\left[1 + S(C+N)R\right]} \right\}, \quad \left(0 \le w \le \infty \right) \tag{3.58}$$

The *Pd* for the CA CFAR detector with the specified number of reference cells *2N* is given as

$$P_d = \int_0^\infty \left(\int_t^\infty p_{w+s}(w)\, dw \right) p(t_{CA})\, dt_{CA}$$

$$= \left[1 + \frac{\beta}{2N\left(1 + S(C+N)R\right)} \right]^{-2N\,'} \tag{3.59}$$

and for the ideal single pulse fixed threshold detection

$$P_{d_{ideal\ fixed}} = \int_t^\infty p_{w+s}(w)\, dw = \exp\left(-\frac{\beta_{ideal\ fixed}}{1 + S(C+N)R} \right) \tag{3.60}$$

For the specified values of *Pd* and a given *Pfa*, provided by appropriate choice of β in the CA CFAR detector with the specified number of reference cells *2N*, the required *S(C+N)R* is determined from (3.59).

For the same values of *Pd* and *Pfa*, provided by appropriate choice of $\beta_{idealfixed}$, the required *S(C+N)R* for the ideal fixed threshold detection is determined from (3.60).

Finding the difference between these values of the required *S(C+N)R*, the CFAR loss of the mean clutter plus noise level estimation for the basic CA CFAR detector in Rayleigh clutter plus noise is determined as (in dB) [3] [2, 5]

$$L_{CA}(2N) = -10\log_{10}\left[\frac{\left(\dfrac{P_{fa}^{-1/2N} - 1}{P_d^{-1/2N} - 1} \right) - 1}{\left(\dfrac{\ln(P_{fa})}{\ln(P_d)} \right) - 1} \right] \tag{3.61}$$

According to (3.61), the larger is the number of reference cells in the CA CFAR detector, the smaller is the value of CFAR loss of mean level estimation in the conditions of spatially uncorrelated homogeneous Rayleigh-distributed clutter plus noise mixture.

---

[3] It has been noted that CFAR loss is roughly constant among the Swerling fluctation models including the non-fluctuating target case.

3.4.1.2 CFAR Loss of the Mean Level Estimation in Rayleigh Clutter Plus Noise Mixture for a GO CFAR Square-law Detector

As the GO CFAR processor was introduced to counter the problem of transitions in clutter power (clutter edges), the additional CFAR loss $\Delta L_{GO}(2N)$ for the GO CFAR detector in Rayleigh clutter plus noise mixture, relative to the basic CA CFAR, when the background clutter plus noise mixture is stationary, can be determined using the results presented in [5, 6].

In homogeneous Rayleigh background, the clutter plus noise level estimates in the early and late windows for single pulse returns are independent with identical chi-square PDFs

$$p(z_E) \;=\; \frac{N^N}{\overline{z}_E^N} \frac{z_E^{N-1}}{\Gamma(N)} \exp\!\left(-\frac{N\,z_E}{\overline{z}_E}\right) \tag{3.62}$$

The CDF of the mean clutter plus noise level estimation after implementing the "greatest of" procedure is then given by

$$F(z_{GO}) \;=\; F(z_E)\,F(z_L)\,, \tag{3.63}$$

where $F(z_E)$ is the CDF corresponding to $p(z_E)$ in (3.62).

The PDF is found by differentiation

$$
\begin{aligned}
p(z_{GO}) &= \frac{dF(z_{GO})}{dz_{GO}} \;=\; 2\,p(z_E)F(z_E) \\[2mm]
&= 2\,\frac{N^N}{\overline{z}_{GO}^N}\frac{z_{GO}^{N-1}}{\Gamma(N)}\exp\!\left(-\frac{Nz_{GO}}{\overline{z}_{GO}}\right)\int_0^{z_{GO}} \frac{N^N}{\overline{z}_{GO}^N}\frac{s^{N-1}}{\Gamma(N)}\exp\!\left(-\frac{Ns}{\overline{z}_{GO}}\right)ds \\[2mm]
&= 2\,\frac{N^N}{\overline{z}_{GO}^N}\frac{z_{GO}^{N-1}}{\Gamma(N)}\exp\!\left(-\frac{Nz_{GO}}{\overline{z}_{GO}}\right)\gamma\!\left(N,\frac{Nz_{GO}}{\overline{z}_{GO}}\right)
\end{aligned}
\tag{3.64}
$$

The incomplete Gamma function in (3.64) can be expressed as a finite series expansion:

$$\gamma\!\left(N,\frac{Nz_{GO}}{\overline{z}_{GO}}\right) \;=\; \Gamma(N)\left[1-\exp\!\left(-\frac{Nz_{GO}}{\overline{z}_{GO}}\right)\sum_{k=0}^{N-1}\left(\frac{Nz_{GO}}{\overline{z}_{GO}}\right)^k\frac{1}{k!}\right] \tag{3.65}$$

Therefore, the GO CFAR threshold, t_{GO}, will have a distribution given by

$$p(t_{GO}) = 2 \frac{N^N}{\overline{z}_{GO}^N} \frac{t_{GO}^{N-1}}{\beta^N} \exp\left(-\frac{Nt_{GO}}{\beta\,\overline{z}_{GO}}\right) \left[1 - \exp\left(-\frac{Nt_{GO}}{\beta\,\overline{z}_{GO}}\right) \sum_{k=0}^{N-1}\left(\frac{Nt_{GO}}{\beta\,\overline{z}_{GO}}\right)^k \frac{1}{k!}\right], \qquad (0 \le t_{GO} \le \infty)$$

(3.66)

Then, the *Pfa* following this threshold is given by

$$P_{fa} = \int_0^\infty \left(\int_t^\infty p(w)\,dw\right) p(t_{GO})\,dt_{GO}$$

$$= 2\left[\left(1 + \frac{\beta}{N}\right)^{-N} - \left(2 + \frac{\beta}{N}\right)^{-N} \sum_{k=0}^{N-1}\binom{N-1+k}{k}\left(2 + \frac{\beta}{N}\right)^{-k}\right]$$

(3.67)

For single pulse square-law detection, the *Pd* of a Swerling 2 target with a given *S(C+N)R* at the input of the GO CFAR detector having the specified number of reference cells *2N* is given as

$$P_d = \int_0^\infty \left(\int_t^\infty p_{w+s}(w)\,dw\right) p(t_{GO})\,dt_{GO} = 2\left[\left(1 + \frac{\beta}{N\left(1 + S(C+N)R\right)}\right)^{-N}\right.$$

$$\left. - \left(2 + \frac{\beta}{N\left(1 + S(C+N)R\right)}\right)^{-N} \sum_{k=0}^{N-1}\binom{N-1+k}{k}\left(2 + \frac{\beta}{N\left(1 + S(C+N)R\right)}\right)^{-k}\right]$$

(3.68)

For the specified values of *Pd* and a given *Pfa*, provided by appropriate choice of β in the GO CFAR detector with the specified number of reference cells *2N*, the required *S(C+N)R* is determined from (3.68). For the same values of *Pd* and *Pfa* the required *S(C+N)R* for the CA CFAR detector is determined from (3.59). Finding the difference between these values of the required *S(C+N)R*, the additional CFAR loss of the mean clutter plus noise level estimation $\Delta L_{GO}(2N)$ for the GO CFAR detector in homogeneous Rayleigh clutter plus noise mixture, relative to the CA CFAR, can be determined.

Figure 17 shows the dependencies of the additional CFAR loss $\Delta L_{GO}(2N)$ due to the "greatest of" selection on the number of reference cells for several values of the required *Pfa*. It can be seen that the additional CFAR loss $\Delta L_{GO}(2N)$ is quite small in homogeneous Rayleigh clutter plus noise mixture, and typically falls in the range of 0.1 to 0.3 dB [5]. Thus, in homogeneous Rayleigh clutter plus noise mixture the GO CFAR processor exhibits minor additional degradation in performance compared with the CA CFAR processor.
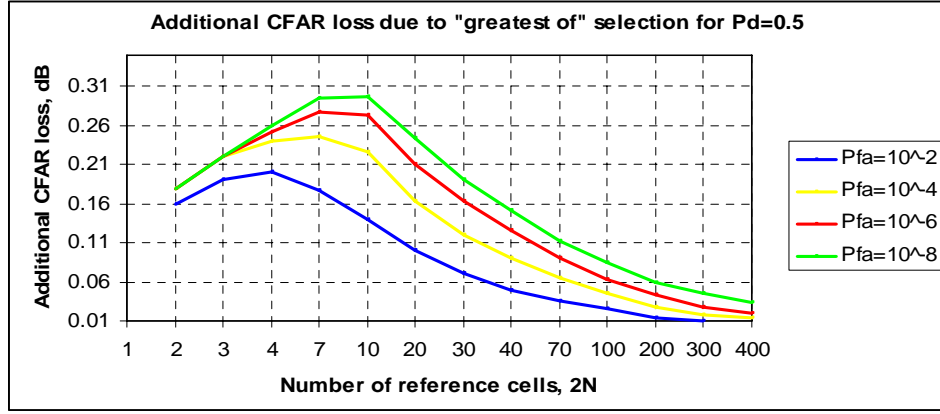
Figure 17: Additional CFAR loss due to "greatest of" selection in Rayleigh clutter plus noise mixture for Pd = 0.5.

3.4.1.3 CFAR Loss of the Mean Level Estimation in Rayleigh Clutter Plus Noise Mixture for a SO CFAR Square-law Detector

As the SO-CFAR detector has been recommended in order to improve resolution of closely spaced targets, the additional CFAR loss $\Delta L_{SO}(2N)$ for the SO CFAR detector in homogeneous Rayleigh clutter plus noise mixture, relative to the basic CA CFAR without an interfering target, can be determined using the results presented in [7].

In homogeneous Rayleigh background, the clutter plus noise level estimates in the early and late windows for single pulse returns are independent with identical chi-square PDFs

$$p(z_E) \;=\; \frac{N^N}{\overline{z}_E^N} \, \frac{z_E^{N-1}}{\Gamma(N)} \, \exp\!\left(-\frac{N z_E}{\overline{z}_E}\right) \tag{3.69}$$

The CDF of the mean clutter plus noise level estimation after implementing the "smallest of" procedure is then given by

$$F(z_{SO}) \;=\; F(z_E) + F(z_L) - F(z_E)F(z_L) \tag{3.70}$$

The PDF is found by differentiation

$$
\begin{aligned}
p(z_{SO}) \;=\; \frac{dF(z_{SO})}{dz_{SO}} \;&=\; 2\,p(z_E)\big[1 - F(z_L)\big] \\
&=\; 2\,p(z_E) - 2\,p(z_E)F(z_L) \\
&=\; 2\,p(z_E) - p(z_{GO})
\end{aligned}
\qquad , \tag{3.71}
$$

where $F(z_E)$ is the CDF corresponding to $p(z_E)$ in (3.69).

Thus,

$$p(z_{SO}) = 2\frac{N^N}{\overline{z}_{SO}^N}\frac{z_{SO}^{N-1}}{\Gamma(N)}\exp\left(-\frac{Nz_{SO}}{\overline{z}_{SO}}\right) - 2\frac{N^N}{\overline{z}_{SO}^N}\frac{z_{SO}^{N-1}}{\Gamma(N)}\exp\left(-\frac{Nz_{SO}}{\overline{z}_{SO}}\right)\gamma\left(N,\frac{Nz_{SO}}{\overline{z}_{SO}}\right) \quad (3.72)$$

Therefore, the SO CFAR threshold, t_{SO}, will have a distribution given by

$$p(t_{SO}) = 2\frac{N^N}{\overline{z}_{SO}^N}\frac{t_{SO}^{N-1}}{\beta^N}\exp\left(-\frac{Nt_{SO}}{\beta\overline{z}_{SO}}\right)\left\{\frac{1}{\Gamma(N)} - \left[1-\exp\left(-\frac{Nt_{SO}}{\beta\overline{z}_{SO}}\right)\sum_{k=0}^{N-1}\left(\frac{Nt_{SO}}{\beta\overline{z}_{SO}}\right)^k\frac{1}{k!}\right]\right\}$$

$$(3.73)$$

$$for \quad (0 \le t_{SO} \le \infty)$$

Then, the *Pfa* corresponding to this threshold is given by

$$P_{fa} = \int_0^\infty\left(\int_t^\infty p(w)\,dw\right)p(t_{SO})\,dt_{SO} = 2\left(2+\frac{\beta}{N}\right)^{-N}\sum_{k=0}^{N-1}\binom{N-1+k}{k}\left(2+\frac{\beta}{N}\right)^{-k} \quad (3.74)$$

For single pulse square-law detection, the *Pd* of a Swerling 2 target with a given *S(C+N)R* at the input of the SO CFAR detector having the specified number of reference cells 2*N* is given as

$$P_d = \int_0^\infty\left(\int_t^\infty p_{w+s}(w)\,dw\right)p(t_{SO})\,dt_{SO}$$

$$= 2\left(2+\frac{\beta}{N(1+S(C+N)R)}\right)^{-N}\sum_{k=0}^{N-1}\binom{N-1+k}{k}\left(2+\frac{\beta}{N(1+S(C+N)R)}\right)^{-k} \qquad (3.75)$$

For the specified values of *Pd* and a given *Pfa*, provided by appropriate choice of β in the SO CFAR detector with the specified number of reference cells 2*N*, the required *S(C+N)R* is determined from (3.75). For the same values of *Pd* and *Pfa* the required *S(C+N)R* for the CA CFAR detector is determined from (3.59). Finding the difference between these values of the required *S(C+N)Rs*, the additional CFAR loss of the mean clutter plus noise level estimation $\Delta L_{GO}(2N)$ for the GO CFAR detector, in homogeneous Rayleigh clutter plus noise, relative to the CA CFAR can be determined. The values of the additional CFAR loss $\Delta L_{SO}(2N)$ due to "smallest of" selection, relative to the basic CA CFAR without an interfering target, are presented in Table 5 [7]. It is clearly seen that in homogeneous Rayleigh clutter plus noise mixture $\Delta L_{SO}(2N)$ is quite large for a small number of reference cells, and that as the number of reference cells increases, the loss asymptotically vanishes.

Table 5: SO CFAR additional CFAR loss $\Delta L_{SO}(2N)$ versus number of reference cells 2N and Pfa without an interfering target, Pd=0.5.

Pfa	$\Delta L_{SO}(2N)$, dB			
	2N=4	2N=8	2N=16	2N=32
10^{-4}	6.63	2.58	0.99	0.41
10^{-6}	16.3	4.51	1.76	0.70
10^{-8}	16.2	6.69	2.64	1.05

It can be concluded that the SO CFAR should not be used unless the number of reference cells is large enough.

Thus, analysing the results presented in Section 3.5.1, it can be concluded that in the noise-limited detection region the CFAR processing with a long cell-averaging length is optimal.

3.4.2 CFAR Loss of the Mean Level Estimation in Non-Rayleigh Clutter Plus Noise Mixture

The following sections of the report present the results of analysis of the CFAR loss of the mean clutter plus noise level estimation for the CA, GO and SO CFAR detectors for different spatial correlation properties of non-Rayleigh clutter and noise mixture.

The CFAR performance in non-Rayleigh clutter plus noise mixture can be derived in an equivalent manner to that for Rayleigh clutter plus noise mixture. However, such a mathematical analysis is very difficult to implement. Consequently, the results are obtained by using a combination of simulation and mathematical analysis, based on the compound formulation of the K-distributed clutter model.

3.4.2.1 *CFAR Loss of the Mean Level Estimation in Spatially Uncorrelated and Weakly Correlated Non-Rayleigh Clutter Plus Noise Mixture*

The CFAR processor of the high-resolution ASW mode is expected to work with uncorrelated non-Rayleigh (or weakly correlated) clutter plus noise mixture samples when clutter is received from low grazing angles in conditions of calm sea, when the sea structure is not well developed. Such a situation is typical for the clutter-limited and the intermediate detection performance regions in conditions of non-equilibrium (developing/decaying) low and medium sea states, when no swell is observed. The same correlation properties of clutter plus noise mixture are expected for the intermediate detection region in conditions of a fully developed low sea states, as the correlation features of the overall clutter plus noise mixture would be determined mostly by the strong noise influence.

In general, the analysis of the CFAR loss of the mean level estimation in spatially uncorrelated and weakly correlated K-distributed clutter plus noise mixture for any CFAR processor has to be performed as follows [14]:

1. The PDF of the test statistic z, $p(z)$, has to be found for the CFAR processor type under consideration that has the specified number of reference cells $2N$.

    a. For the CA, GO and SO CFAR detectors the PDFs of the test statistic z, $p(z)$, are determined as follows:

    For the CA CFAR detector, p(zCA) is obtained from the 2N-fold convolution of the clutter plus noise PDF $p(w)$ (3.11) with itself, and cannot be represented in closed form;

    b. For the GO CFAR detector, p(zGO) is given by

    $$p\left(z_{GO}\right) \;=\; \frac{dF\left(z_{GO}\right)}{dz_{GO}} \;=\; 2\,p\left(z_E\right)F\left(z_E\right), \tag{3.76}$$

    where $F(z_E)$ is the CDF of $p(z_E)$, and $p(z_E)$ is the PDF of the clutter plus noise level estimates in the early or later windows for single pulse returns that is obtained from the N-fold convolution of the clutter plus noise PDF $p(w)$ (3.11) with itself.

    c. For the SO CFAR detector, p(zSO) is given by

    $$p\left(z_{SO}\right) \;=\; \frac{dF(z_{SO})}{dz_{SO}} \;=\; 2\,p\left(z_E\right)\left[1-F\left(z_L\right)\right], \tag{3.77}$$

    where $F(z_L)$ is the CDF of $p(z_E)$, and $p(z_E)$ is the PDF of the clutter plus noise level estimates in the early or later windows for single pulse returns that is obtained from the N-fold convolution of the clutter plus noise PDF $p(w)$ (3.11) with itself.

2. The *Pfa* for the CFAR detector type under consideration that has the specified number of reference cells $2N$, has to be obtained from

$$P_{fa} \;=\; \int_0^\infty \left[\int_0^\infty \exp\left(-\frac{\beta\,z}{2\sigma^2+(4y^2/\pi)}\right)\frac{2b^{2\nu}}{\Gamma(\nu)}\,y^{2\nu-1}\,\exp\left(-b^2\,y^2\right)dy\right]p(z)\,dz, \tag{3.78}$$

3. The Pd of a Swerling 2 target for the CFAR detector type under consideration that has the specified number of reference cells 2N, may be obtained from:

$$P_d \;=\; \int_0^\infty \left[\int_0^\infty \exp\left(-\frac{\beta\,z}{2\sigma^2+4y^2/\pi+\overline{A}^2/2}\right)\frac{2b^{2\nu}}{\Gamma(\nu)}\,y^{2\nu-1}\exp\left(-b^2\,y^2\right)dy\right]p(z)\,dz, \tag{3.79}$$

4. For the specified values of Pd and a given Pfa, provided by appropriate choice of β in the CFAR detector with the specified number of reference cells 2N under consideration, the required S(C+N)R may be determined from (3.79). For the same values of Pd and Pfa, provided by appropriate choice of βideal fixed, the required S(C+N)R for "ideal fixed" threshold detection is determined from (3.17). Finding the difference between these values of the required S(C+N)R, the

CFAR loss of the mean clutter plus noise level estimation, for the CFAR detector in K-distributed clutter plus noise mixture is determined.

However, such a mathematical analysis is very difficult to implement.

It was shown [28] that it is much simpler to analyse the performance of CFAR processors and CFAR loss in K-distributed clutter plus noise mixture, using a combination of simulation and mathematical analysis, based on the compound formulation of the K-distributed clutter model. This allows the PDF of the CFAR threshold to be estimated in K-distributed clutter with specified correlation properties for each individual cell under test by using a simulation of a mixture of Gamma distributed data and noise.

As an example, consider in more detail the performance of the CA CFAR detector with the specified number of reference cells $2N$ in a mixture of K-distributed clutter and noise. For a given observation region with underlying mean intensity of the clutter values $\frac{4}{\pi} y_i^2$ and mean level of noise, $2\sigma^2$, the threshold, t_{CA}, can be regarded as a randomly distributed variable.

From the central limit theorem, for the CA CFAR detector the distribution of t_{CA} will become approximately Gaussian, especially for a large number of samples. The expected value of t_{CA} will be the mean of the summed random variates (with the distribution parameters determined by (3.10))

$$m_t = \hat{\beta} \sum_{i=1}^{2N} \frac{w_i}{2N} = \hat{\beta} \sum_{i=1}^{2N} \frac{1}{2N} \left(2\sigma^2 + \frac{4}{\pi} y_i^2 \right) \qquad (3.80)$$

The variance of the threshold will be the sum of the variances of the $2N$ random variates (partly correlated or uncorrelated)

$$\sigma_t^2 = \hat{\beta}^2 \, 2N \left\{ \sum_{i=1}^{2N} \frac{\xi_i^4}{(2N)^2} + 2 \sum_{j=1}^{2N-1} \rho_j \sum_{i=1}^{2N-j} \frac{\xi_i^2 \xi_{j+i}^2}{(2N)^2} \right\} , \qquad (3.81)$$

where $\xi_i^2 = 2\sigma^2 + \frac{4}{\pi} y_i^2$ and ρ_j is the appropriate correlation coefficient, which is determined by the radar pulse length τ_P and the sampling interval τ_S ($\rho_j = 0$ if $\tau_P \leq \tau_S$).

The PDF of the threshold $p(t_{CA})$ in the mixture of K-distributed clutter and noise for a single cell under test is then

$$p(t_{CA}) = \frac{1}{\sqrt{2\pi}\sigma_t} \exp\left(\frac{(t-m_t)^2}{2\sigma_t^2} \right); \qquad 0 \leq t \leq \infty \qquad (3.82)$$

The simulation of noise and uncorrelated (or correlated) Chi-distributed variates y_j (as described, for example, in [22, 29]) with the required shape ν and scale b parameters, that are dependent on the statistical properties of clutter in the analysed CFAR area, allows values of m_t and σ_t to be estimated for successive cells under test. From these, the successive PDFs of the threshold in a mixture of K-distributed clutter and noise (with the mean level of $2\sigma^2$) can be produced, allowing the calculation of the *Pfa* and *Pd* for each cell under test and for the overall range profile. The *Pfa* and *Pd* are then available as functions of range (along the profile), as well as the averaged values for the profile.

For single pulse detection in each scan

$$\left[P_{fa}(y_j,1) \right]_{CA} = \int_0^\infty p(t_{CA})\, P_{fa}(y_j,1,t_{CA})\, dt_{CA}$$

$$= \int_0^\infty \frac{1}{\sqrt{2\pi}\,\sigma_t} \exp\left(-\frac{(t_{CA}-m_t)^2}{2\sigma_t^2} \right) \int_{t_{CA}}^\infty \frac{1}{2\sigma^2 + (4y_j^2/\pi)} \exp\left(-\frac{w}{2\sigma^2 + (4y_j^2/\pi)} \right) dw\, dt_{CA}$$

$$= \frac{1}{\sqrt{2\pi}\,\sigma_t} \int_0^\infty \exp\left(-\frac{(\beta z_{CA}-m_t)^2}{2\sigma_t^2} - \frac{\beta z_{CA}}{2\sigma^2 + (4y_j^2/\pi)} \right) dt_{CA} \qquad (3.83)$$

where $P_{fa}(y_j,1,t_{CA})$ is the *Pfa* for a sample with clutter of mean level y_j and noise of variance σ^2, with a threshold t_{CA}

$$P_{fa}\left(y_j, 1, t_{CA} \right) = \int_{t_{CA}}^\infty \frac{1}{2\sigma^2 + (4y_j^2/\pi)} \exp\left(-\frac{w}{2\sigma^2 + (4y_j^2/\pi)} \right) dw$$

$$= \exp\left(-\frac{t_{CA}}{2\sigma^2 + (4y_j^2/\pi)} \right) \qquad (3.84)$$

$$= \exp\left(-\frac{\beta z_{CA}}{2\sigma^2 + (4y_j^2/\pi)} \right)$$

The mean clutter level y_j, and the CFAR threshold t_{CA} will vary with successive data samples. This results in an equivalent variation of the *Pfa*.

The value of $\left\lfloor P_{fa}(y_j,1) \right\rfloor_{CA}$ should be calculated for each position of the window, over the range profile generated for the CFAR area and then averaged to give the overall value of the *Pfa* for that profile

$$\left[\bar{P}_{fa} \right]_{CA} = \frac{1}{J} \sum_{j=1}^J \left[P_{fa}\left(y_j, 1 \right) \right]_{CA} \qquad (3.85)$$

47

where J is the number of samples of the underlying mean level y.

The calculation of Pd for a sample of a target in a mixture of K-distributed sea clutter and noise follows a similar approach to that given in equation (3.83).

The Pd averaged over the threshold distribution $p(t_{CA})$, $\left[P_d(y_j, A, 1)\right]_{CA}$, is given in each scan by

$$\left[P_d(y_j, A, 1)\right]_{CA} = \int_0^\infty p(t_{CA})\, P_d(y_j, A, 1, t_{CA})\, dt_{CA} \tag{3.86}$$

where $P_d(y_j, A, 1, t_{CA})$ is the Pd for a sample with amplitude of the reflected target signal A in mixture of clutter with mean level y_j and noise with variance σ^2, with a threshold t_{CA}.

Therefore, for the Swerling 2 target characteristics the single pulse detection probability $\left[P_d(y_j, A, 1)\right]_{CA}$ is given by

$$
\begin{aligned}
\left[P_d(y_j, A, 1)\right]_{CA} &= \int_0^\infty p(t_{CA})\, P_d(y_j, A, 1, t_{CA})\, dt_{CA} \\
&= \int_0^\infty \frac{1}{\sqrt{2\pi}\sigma_t} \exp\left(-\frac{(t_{CA}-m_t)^2}{2\sigma_t^2}\right) \int_{t_{CA}}^\infty \frac{1}{2\sigma^2 + 4y_j^2/\pi + \overline{A}^2} \exp\left(-\frac{w}{2\sigma^2 + 4y_j^2/\pi + \overline{A}^2}\right) dw\, dt_{CA} \\
&= \frac{1}{\sqrt{2\pi}\sigma_t} \int_0^\infty \exp\left(-\frac{(t_{CA}-m_t)^2}{2\sigma_t^2}\right) \exp\left(-\frac{t_{CA}}{2\sigma^2 + 4y_j^2/\pi + \overline{A}^2}\right) \tag{3.87}
\end{aligned}
$$

where $P_d(y_j, A, 1, t_{CA})$ is the probability of a single pulse detection for the cell under test with a mean level y_j, when the amplitude of target is characterised by the parameter A and with a fixed threshold t_{CA} determined as

$$
\begin{aligned}
P_d\left(y_j, A, 1, t_{CA}\right) &= \int_t^\infty \frac{1}{2\sigma^2 + (4y_j^2/\pi) + \overline{A}^2} \exp\left(-\frac{w}{2\sigma^2 + (4y_j^2/\pi) + \overline{A}^2}\right) dw \\
&= \exp\left(-\frac{t_{CA}}{2\sigma^2 + (4y_j^2/\pi) + \overline{A}^2}\right) \tag{3.88} \\
&= \exp\left(-\frac{\beta\, z_{CA}}{2\sigma^2 + (4y_j^2/\pi) + \overline{A}^2}\right)
\end{aligned}
$$

The overall value of the Pd for the CFAR area is the average over all data samples of the individual values obtained

$$\left[\bar{P}_d \right]_{CA} = \frac{1}{J} \sum_{j=1}^{J} \left[P_d \left(y_j, A, 1 \right) \right]_{CA} \tag{3.89}$$

Then, for the specified values of *Pd* and a given *Pfa*, provided by appropriate choice of β in the CA CFAR detector with the specified number of reference cells *2N*, the required *S(C+N)R* is determined from (3.89). For the same values of *Pd* and *Pfa*, provided by appropriate choice of $\beta_{ideal\ fixed}$, the required *S(C+N)R* for "ideal fixed" threshold detection is determined from (3.17). The CFAR loss of the mean clutter plus noise level estimation for the CA CFAR detector in K-distributed clutter plus noise mixture can be determined as the difference between these values of the required *S(C+N)R*.

A similar simplified analysis can be implemented for the GO and SO CFAR detectors in order to estimate the values of CFAR loss of the mean clutter plus noise level estimation. If the number of reference cell on either side of the test cell is *N*, the PDFs of the sums in earlier and later windows for these detectors in the mixture of K-distributed clutter and noise are given

$$p(z_E) = \frac{1}{\sqrt{2\pi}\sigma_E} \exp\left(\frac{(z_E - m_E)^2}{2\sigma_E^2} \right); \qquad 0 \le z_E \le \infty \tag{3.90}$$

where the expected value of z_E is the mean of the summed random variates (with the distribution parameters determined by (3.10))

$$m_E = \sum_{i=1}^{N} \frac{w_i}{N} = \sum_{i=1}^{N} \frac{1}{N} \left(2\sigma^2 + \frac{4}{\pi} y_i^2 \right) \tag{3.91}$$

and the variance of z_E is the sum of the variances of the *N* random variates (partly correlated or uncorrelated)

$$\sigma_E^2 = N \left\{ \sum_{i=1}^{N} \frac{\xi_i^4}{(N)^2} + 2 \sum_{j=1}^{N-1} \rho_j \sum_{i=1}^{N-j} \frac{\xi_i^2 \xi_{j+i}^2}{(N)^2} \right\} \tag{3.92}$$

Then, the PDF of the test statistic $p_{GO}(z)$ is determined as

$$\begin{aligned} p\left(z_{GO} \right) &= 2\, p\left(z_E \right) F\left(z_E \right) \\ &= \frac{2}{\sqrt{2\pi}\sigma_E} \exp\left(\frac{(z_{GO} - m_E)^2}{2\sigma_E^2} \right) \int_0^{z_{GO}} \frac{1}{\sqrt{2\pi}\sigma_E} \exp\left(\frac{(s - m_E)^2}{2\sigma_E^2} \right) ds \\ &= \frac{1}{\sqrt{2\pi}\sigma_E} \exp\left(\frac{(z_{GO} - m_E)^2}{2\sigma_E^2} \right) Erf\left[\frac{z_{GO} - m_E}{\sqrt{2}\sigma_E} \right] \end{aligned} \tag{3.93}$$

Therefore, the PDF of the threshold $p(t_{GO})$ in the mixture of K-distributed clutter and noise for a single cell under test is given by

$$p(t_{GO}) = \frac{1}{\sqrt{2\pi}\,\beta\sigma_E}\exp\left(\frac{(t_{GO}-\beta m_E)^2}{2\beta^2\sigma_E^2}\right)Erf\left[\frac{t_{GO}-\beta m_E}{\sqrt{2}\,\beta\sigma_E}\right] \tag{3.94}$$

The PDF of the test statistic $p_{SO}(z)$ is obtained as

$$p(z_{SO}) = 2p(z_E)\left[1-F(z_L)\right]$$

$$= \frac{2}{\sqrt{2\pi}\sigma_E}\exp\left(\frac{(z_{SO}-m_E)^2}{2\sigma_E^2}\right)\left[1-\int_0^{z_{SO}}\frac{1}{\sqrt{2\pi}\sigma_E}\exp\left(\frac{(s-m_E)^2}{2\sigma_E^2}\right)ds\right]$$

$$= \frac{2}{\sqrt{2\pi}\sigma_E}\exp\left(\frac{(z_{SO}-m_E)^2}{2\sigma_E^2}\right)-\frac{1}{\sqrt{2\pi}\sigma_E}\exp\left(\frac{(z_{SO}-m_E)^2}{2\sigma_E^2}\right)Erf\left[\frac{z_{SO}-m_E}{\sqrt{2}\sigma_E}\right] \tag{3.95}$$

Hence, the PDF of the threshold $p(t_{SO})$ in the mixture of K-distributed clutter and noise for a single cell under test is given by

$$p(t_{SO}) = \frac{2}{\sqrt{2\pi}\,\beta\sigma_E}\exp\left(\frac{(t_{SO}-\beta m_E)^2}{2\beta^2\sigma_E^2}\right)-\frac{1}{\sqrt{2\pi}\beta\sigma_E}\exp\left(\frac{(t_{SO}-\beta m_E)^2}{2\beta^2\sigma_E^2}\right)Erf\left[\frac{t_{SO}-\beta m_E}{\sqrt{2}\,\beta\sigma_E}\right] \tag{3.96}$$

Using (3.94) and (3.96), the calculation of *Pfa* and *Pd* for each cell under test and for the overall range profile for both the GO and SO CFAR detectors can be implemented:

1. GO CFAR detector

$$\left[\bar{P}_{fa}\right]_{GO} = \frac{1}{J}\sum_{j=1}^{J}\int_0^{\infty}p(t_{GO})\,P_{fa}(y_j,1,t_{GO})\,dt_{GO}$$

$$= \frac{1}{J}\sum_{j=1}^{J}\int_0^{\infty}p(t_{GO})\exp\left(-\frac{t_{GO}}{2\sigma^2+(4y_j^2/\pi)}\right)dt_{GO} \tag{3.97}$$

$$\left[\bar{P}_d\right]_{GO} = \frac{1}{J}\sum_{j=1}^{J}\int_0^{\infty}p(t_{GO})\,P_d(y_j,1,t_{GO})\,dt_{GO}$$

$$= \frac{1}{J}\sum_{j=1}^{J}\int_0^{\infty}p(t_{GO})\exp\left(-\frac{t_{GO}}{2\sigma^2+(4y_j^2/\pi)+\bar{A}^2}\right)dt_{GO} \tag{3.98}$$

2. SO CFAR detector

$$\left[\bar{P}_{fa}\right]_{SO} = \frac{1}{J}\sum_{j=1}^{J}\int_{0}^{\infty} p(t_{SO})\, P_{fa}(y_j,1,t_{SO})dt_{SO}$$

$$= \frac{1}{J}\sum_{j=1}^{J}\int_{0}^{\infty} p(t_{SO})\exp\left(-\frac{t_{SO}}{2\sigma^2+(4y_j^2/\pi)}\right)dt_{SO}$$

(3.99)

$$\left[\bar{P}_{d}\right]_{SO} = \frac{1}{J}\sum_{j=1}^{J}\int_{0}^{\infty} p(t_{SO})\, P_{d}(y_j,1,t_{SO})\,dt_{SO}$$

$$= \frac{1}{J}\sum_{j=1}^{J}\int_{0}^{\infty} p(t_{SO})\exp\left(-\frac{t_{SO}}{2\sigma^2+(4y_j^2/\pi)+\bar{A}^2}\right)dt_{SO}$$

(3.100)

Then, for the specified values of *Pd* and a given *Pfa*, provided by appropriate choice of β in the GO CFAR detector with the specified number of reference cells *2N*, the required *S(C+N)R* is determined from (3.98). For the specified values of *Pd* and a given *Pfa*, provided by appropriate choice of β in the SO CFAR detector with the specified number of reference cells *2N*, the required *S(C+N)R* is determined from (3.100). For the same values of *Pd* and *Pfa*, provided by appropriate choice of $\beta_{ideal\ fixed}$, the required *S(C+N)R* for "ideal fixed" threshold detection is determined from (3.17). Finding the difference between the corresponding values of the required *S(C+N)Rs*, the CFAR loss of the mean clutter plus noise level estimation for the GO and SO CFAR detectors in K-distributed clutter plus noise mixture can be determined.

As discussed in Section 3.2 of the report, the presence of thermal noise in the radar receiver, which in general cannot be neglected, modifies the distribution of the received signals. The lower the *CNR*, the closer the amplitude distribution of a mixture of K-distributed sea clutter with noise gets to a Rayleigh distribution. Therefore, the value of CFAR loss for any CFAR detector is determined not only by the CFAR processor design and the required *Pd* and *Pfa*, as it is for Rayleigh clutter plus noise mixture, but by the clutter shape parameter and *CNR* as well. A reasonable guide to radar performance prediction for single pulse detection is to represent the received signal, which is a mixture of K-distributed sea clutter with a shape parameter ν and non-negligible noise, as being K-distributed with a modified effective shape parameter ν_{eff} (3.20).

Table 6 presents the results of calculation of the CFAR loss of the mean clutter plus noise level estimation in uncorrelated spiky clutter [7]. These results provide the CFAR loss of the mean clutter plus noise level estimation for the CA CFAR, GO CFAR and ordered statistics (OS) CFAR processors. Note that the OS CFAR detector serves the same purpose as the SO CFAR detector, but has a lower CFAR loss. The first column, labelled as $L_{ideal\ fixed}$, gives the loss associated with ideal fixed threshold detection in spiky K-distributed clutter compared to the detection in Rayleigh clutter plus noise mixture.

Table 6: CFAR loss of the mean level estimation of spatially uncorrelated non-Rayleigh clutter plus noise mixture for Pd = 0.5 and Pfa = 10⁻⁶ .

		L_{CA} , dB		L_{GO} , dB		L_{OS} , dB	
		2N=16	2N=32	2N=16	2N=32	2N=16	2N=32
v_{eff} = 0. 10	13.95	19.49	8.20	19.73	10.00	34.78	17.33
v_{eff} = 0. 25	10.83	7.43	3.52	7.73	3.87	11.68	5.48
v_{eff} = 0. 50	8.59	4.24	2.07	4.67	2.38	6.10	3.02
v_{eff} = 1.50	5.42	2.50	1.24	2.80	1.45	3.50	1.77
v_{eff} = 9.50	1.83	2.13	1.05	2.37	1.22	2.96	1.45
v_{eff} = ∞	0	2.12	1.04	2.35	1.20	2.93	1.44

It can be seen that a CFAR loss of greater than 2dB can commonly be expected in spiky uncorrelated clutter, with much greater losses of up to tens of decibels being possible in extreme cases of very spiky uncorrelated clutter and small number of reference cells. The advantage of using a large number of reference cells can also be seen to be more pronounced for low values of v_{eff}, where the use of only 16 as opposed to 32 reference cells can introduce an additional loss of 2dB to 5dB under most reasonable conditions, and more in extreme cases.

Table 7 presents the estimated values of an additional CFAR loss of the mean clutter plus noise estimation for the GO and SO CFAR processors relative to the CA CFAR processor in uncorrelated spiky clutter. Note that the K-distribution with v_{eff} = ∞ corresponds to the Rayleigh distribution, and that the K-distribution is effectively Rayleigh for v_{eff} > 20. It can be seen that in uncorrelated spiky clutter the SO CFAR processor suffers much greater loss compared to the GO and CA CFAR processors, especially for a small number of reference cells. The CFAR loss of the mean clutter plus noise level estimation is a strong function of the effective shape parameter for all considered CFAR processors, becoming larger as clutter plus noise mixture becomes spikier (i.e. for smaller values of the effective shape parameter, v_{eff}). The similar values of CFAR loss are expected in weakly correlated non-Rayleigh clutter [24, 28].

Table 7: Additional CFAR loss of the mean level estimation of spatially uncorrelated non-Rayleigh clutter plus noise mixture for Pd = 0.5 and Pfa = 10⁻⁶ for the GO and SO CFAR processors.

	L_{CA} , dB		ΔL_{GO} , dB		ΔL_{SO} , dB	
	2N=16	2N=32	2N=16	2N=32	2N=16	2N=32
v_{eff} = 0. 10	19.49	8.20	0.24	1.80	16.24	9.43
v_{eff} = 0. 25	7.43	3.52	0.30	0.35	5.20	2.26
v_{eff} = 0. 50	4.24	2.07	0.43	0.31	2.81	1.25
v_{eff} = 1.50	2.50	1.24	0.30	0.21	1.95	0.83
v_{eff} = 9.50	2.13	1.05	0.24	0.17	1.78	0.71
v_{eff} = ∞	2.12	1.04	0.23	0.16	1.76	0.70

Figure 18 illustrates the variation with range of different types of threshold in one scan (no pulse-to-pulse integration). The clutter has a shape parameter of $\nu = 0.5$ and the spatial correlation length of $R_{corr} = 1$. The average Pfa is 10^{-4} and the threshold has been set to give a Pd of 0.5 for a Swerling 2 target in each case.
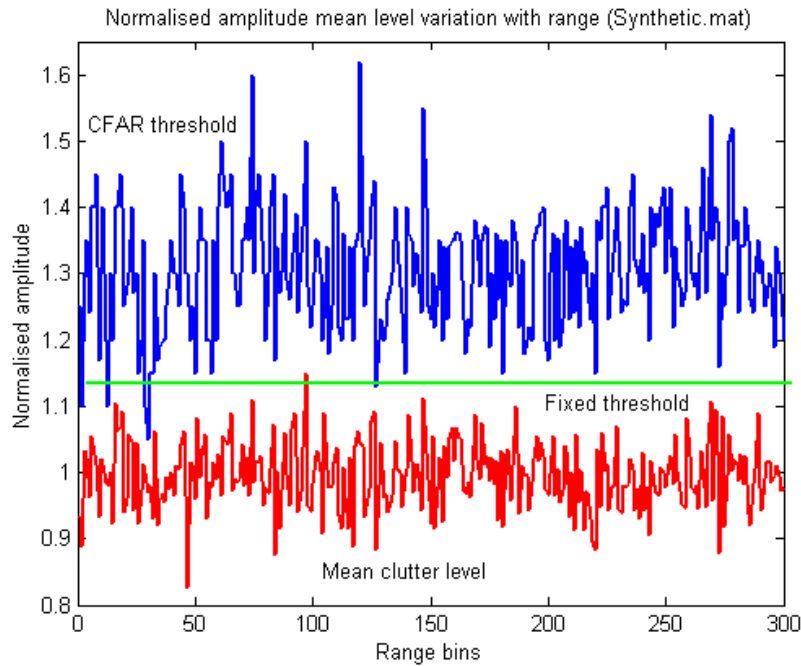
Figure 18: Variation of thresholds with range in weakly correlated K-distributed clutter
        ($R_{cor}= 1$) with $\nu = 0.5$ for average $Pfa=10^{-4}$ (red – mean clutter level for $\nu = 0.5$ and $R_{cor}= 1$; green – ideal fixed threshold; blue - average threshold for a double-sided CA CFAR with N = 5).

It can be seen that, for $R_{corr} = 1$, the average threshold of the 5 +5 cell-average detector is significantly higher than that for the fixed threshold and so a detection loss is to be expected. Thus, for low values of correlation length R_{corr} the CA CFAR performs poorly compared to that of a fixed threshold.

It was shown that [28]:

- The distribution of false alarms in uncorrelated or weakly correlated sea clutter is dominated by occasional regions of high Pfa in both of the cases: fixed threshold and the CFAR threshold with a short cell-averaging length, and

- When there is a little spatial correlation and for relatively high values of ν_{eff} (say, $\nu_{eff} > 5$), the best performance will be obtained from a longer cell-averaging length.

Therefore, the CFAR processing design with a long cell-averaging length is optimal in the clutter-limited and intermediate detection regions in conditions of low and medium sea states, when the sea is not fully developed and swell is not observed.

3.4.2.2 CFAR Loss of the Mean Level Estimation in Strongly Spatially Correlated Non-Rayleigh Clutter Plus Noise Mixture

The CFAR processor of the high-resolution ASW mode is expected to work with strongly spatially correlated non-Rayleigh clutter plus noise mixture samples when sea clutter is received from low grazing angles of the clutter-limited and the intermediate detection regions in conditions of:

- Fully developed medium and high sea states, when the observed swell direction is the same as the wind direction, and

- Non-equilibrium (developing/decaying) seas, when strong swell is observed, and the swell direction is not necessarily the same as the wind direction.

If clutter is strongly spatially correlated, the cell-average detector output is not independent of the cell under test and the CFAR processor performance is affected [13, 14, 28, 38].

For an arbitrary ACF of the mean clutter level, the conditional PDFs of the mean clutter level in the different reference cell, given that in the test cell, will have different variances (depending on their correlation coefficient with the test cell), and will also not be independent due to cross-correlation terms.

To analyse directly the effects of the mixture of noise and correlated K-distributed sea clutter, having the mean clutter level with arbitrary ACF, on CFAR detection performance, the amplitude distribution of such a mixture, is required to determine the PDF of the test statistic $p(z)$.

The CA CFAR processor provides the estimates of the mean clutter plus noise level in the test cell through a combination of $2N$ correlated K-distributed clutter plus noise samples from adjacent reference cells, i.e.

$$\overline{z}_{CA} \;=\; \frac{1}{2N}\sum_{i=1}^{2N} w_i \,, \tag{3.101}$$

For single pulse detection in each scan, the averaged *Pfa*, given the threshold value $t_{CA,}$ is given by

$$\overline{P}_{fa} \;=\; P_{fa}\left(t_{CA}\right) \;=\; \int_0^{\infty} P_{fa}\left(y_0,\,1,\,t_{CA}\right)p\left(y_0\right)dy_0\,, \tag{3.102}$$

where $P_{fa}(y_0,\,1,\,t_{CA})$ is the *Pfa* for a sample with clutter of mean level y_0 and noise of variance σ^2, with a threshold $t_{CA} = \beta\,\overline{z}_{CA}$.

Using the results presented in [15, 16, 23], it can be shown that, assuming an exponential ACF of the spatially correlated mean clutter level, independent speckle

components, and exploiting the Markov property of the mean clutter level amplitude y (Section 3.2.2), the expected value of $P_{fa}(y_0, 1, t_{CA})$ can be presented in the form

$$
P_{fa}(y_0, 1, t_{CA}) = \int_0^\infty ... \int_0^\infty p(y_1, ..., y_{2N}) \frac{-\lambda_0}{\prod_{i=1}^{2N}\left(1 - \frac{\beta\lambda_i}{\lambda_0}\right)} dy_1...dy_{2N} \tag{3.103}
$$

$$
= \int_0^\infty ... \int_0^\infty p(y_2/y_1)...p(y_N/y_0)p(y_0/y_{N+1})...p(y_{2N-1}/y_{2N}) \frac{z_0}{\prod_{i=1}^{2N}\left(1 + \beta\frac{z_i}{z_0}\right)} dy_1...dy_{2N}
$$

where λ_i $(i = 0, 1, 2,..., 2N)$ are the eigenvalues of the clutter plus noise correlation matrix for the CA CFAR processor with $2N$ reference cells, λ_i $(i = 1, 2,..., 2N)$ are the positive eigenvalues corresponding to the mean clutter plus noise intensities in the reference cells $z_i = 2\sigma^2 + 4y_i^2/\pi$ $(i = 1, 2,..., 2N)$, λ_0 is the negative eigenvalue corresponding to the mean clutter plus noise intensity in the test cell $z_0 = 2\sigma^2 + 4y_0^2/\pi$.

Assuming that the early $(i = 1, ..., N)$ and late $(i = N+1, ..., 2N)$ windows consist of the same number of reference cells and their position is symmetrical relative to the cell under the test (i.e. y_i $(i = 1, ..., N)$ is identically distributed to y_{i+N}), the averaged Pfa is determined by

$$
\bar{P}_{fa} =
$$

$$
\int_0^\infty \left(2\sigma^2 + 4y_0^2/\pi\right)p(y_0)\left[\int_0^\infty ... \int_0^\infty p(y_1/y_2)...p(y_N/y_0) \frac{1}{\prod_{i=1}^{N}\left(1 + \beta\frac{2\sigma^2 + 4y_i^2/\pi}{2\sigma^2 + 4y_0^2/\pi}\right)} dy_1...dy_N\right]^2 dy_0,
$$

$$
\tag{3.104}
$$

Then, using (3.104) and (3.98), the averaged Pfa can be presented as

$$
\bar{P}_{fa} = \int_0^\infty S(y_0, \beta)\left(2\sigma^2 + 4y_0^2/\pi\right)p(y_0)dy_0, \tag{3.105}
$$

where

$$S(y_0, \beta) = \left[\frac{1}{b^2(1-p) p^{\frac{v-1}{2}}} \right]^{2N} \frac{1}{y_o^{2(v-1)}} \exp\left(-\frac{py_0^2}{b^2(1-p)} \right) \int_0^\infty \int_0^\infty ... \int_0^\infty \left\{ y_1^{(v-1)} \left[\frac{I_{v-1}\left(\frac{2\sqrt{p}\, y_N y_0}{b^2(1-p)} \right)}{1 + \beta \frac{2\sigma^2 + 4y_N^2/\pi}{2\sigma^2 + 4y_0^2/\pi}} \right] \right.$$

$$\left. * \prod_{i=1}^{N-1} \left[\frac{I_{v-1}\left(\frac{2\sqrt{p}\, y_i y_{i+1}}{b^2(1-p)} \right)}{1 + \beta \frac{2\sigma^2 + 4y_i^2/\pi}{2\sigma^2 + 4y_0^2/\pi}} \right] \exp\left(-\frac{y_1^2 + (1+p)\left(y_2^2 + y_3^2 + ... + y_N^2 \right)}{b^2(1-p)} \right) \right\}^2 dy_1 dy_2 ... dy_N,$$

$$(3.106)$$

Numerical inversion of (3.104) provides the value of threshold multiplier β required for a specified value of *Pfa*, as a function of the correlation of the mean clutter level. Having determined the required value of β, detection probabilities are calculated as follows, for a Swerling 2 target with signal strength $\overline{A}^2$.

Similar to (3.105), for single pulse detection in each scan, the averaged *Pd*, given the threshold value t_{CA}, is given by

$$\overline{P}_d = P_d(t_{CA}) = \int_0^\infty P_d\left(\overline{A}^2, y_0, 1, t_{CA} \right) p(y_0) \, dy_0,$$

$$(3.107)$$

where $P_d(\overline{A}^2, y_0, 1, t_{CA})$ is the *Pd* of a Swerling 2 target for a sample with clutter of mean level y_0 and noise of variance σ^2, with a threshold $t_{CA} = \beta\, \overline{z}_{CA}$.

Using (3.107) and (3.98), the expression for the expected *Pd* of a Swerling 2 target can be presented as

$$\overline{P}_d = \int_0^\infty ... \int_0^\infty p(y_1/y_2) ... p(y_N/y_0) ... p(y_{2N-1}/y_{2N}) p(y_0) *$$

$$\frac{2\sigma^2 + 4y_0^2/\pi}{\prod_{i=1}^{2N} \left(1 + \beta \frac{2\sigma^2 + 4y_i^2/\pi}{2\sigma^2 + 4y_i^2/\pi + \overline{A}^2} \right)} dy_1 ... dy_0 ... dy_{2N}$$

$$(3.108)$$

$$= \int_0^\infty T\left(\overline{A}^2, y_0, \beta \right) \left(2\sigma^2 + 4y_0^2/\pi \right) p(y_0) dy_0$$

where

$$T\left(\bar{A}^2,\, y_0,\, \beta\right) \;=$$

$$\left[\frac{1}{b^2\left(1-p\right)p^{\frac{\nu-1}{2}}}\right]^{2N} \frac{1}{y_o^{2(\nu-1)}} \exp\left(-\frac{py_0^2}{b^2\left(1-p\right)}\right) \int\limits_0^\infty \int\limits_0^\infty \cdots \int\limits_0^\infty \left\{ y_1^{(\nu-1)} \left[\frac{I_{\nu-1}\left(\frac{2\sqrt{p}\,y_N y_0}{b^2\left(1-p\right)}\right)}{1+\beta\,\dfrac{2\sigma^2+4y_N^2\big/\pi}{2\sigma^2+4y_0^2\big/\pi+\bar{A}^2}}\right]\right.$$

$$\left.*\prod_{i=1}^N \left[\frac{I_{\nu-1}\left(\frac{2\sqrt{p}\,y_i y_{i+1}}{b^2\left(1-p\right)}\right)}{1+\beta\,\dfrac{2\sigma^2+4y_i^2\big/\pi}{2\sigma^2+4y_i^2\big/\pi+\bar{A}^2}}\right] \exp\left(-\frac{y_1^2+\left(1+p\right)\left(y_1^2+y_2^2+\cdots+y_N^2\right)}{b^2\left(1-p\right)}\right)\right\}^{2} dy_1 dy_2 \cdots dy_N$$

<div align="right">(3.109)</div>

Then, for the specified values of *Pd* and a given *Pfa*, provided by appropriate choice of *β* in the CA CFAR detector with the specified number of reference cells *2N*, the required *S(C+N)R* is determined from (3.108). For the same values of *Pd* and *Pfa*, provided by appropriate choice of *β*ideal fixed, the required *S(C+N)R* for "ideal fixed" threshold detection is determined from (3.17). Finding the difference between the corresponding values of the required *S(C+N)Rs*, the CFAR loss of the mean clutter plus noise level estimation for the CA CFAR detector in correlated K-distributed clutter plus noise mixture can be determined.

It can be seen that the mathematical analysis of the CFAR loss in correlated K-distributed clutter plus noise mixture is even more difficult to implement than the similar analysis for the uncorrelated K-distributed clutter plus noise case considered in Section 3.5.2.1.

Therefore, the simplified analysis of the CFAR loss of the mean K-distributed spatially correlated clutter plus noise level estimation for any CFAR processor has to be performed in the same way as for the spatially uncorrelated K-distributed clutter plus noise case considered Section 3.5.2.1. The simplified analysis is based on the compound formulation of the K-distributed clutter model and uses a combination of simulation and mathematical analysis, presented by equations (3.70) - (3.90). This allows the PDF of the CFAR threshold to be estimated in K-distributed clutter with prescribed correlation properties for each individual cell under test by using a simulation of a mixture of Gamma distributed data and noise.

The value of CFAR loss of the mean clutter plus noise level estimation depends in the case of correlated K-distributed clutter not only on the type of CFAR processor, the given number of reference cells, the clutter plus noise amplitude distribution

parameters and the required *Pfa* and *Pd*, as it is for the uncorrelated K-distributed clutter case, but on the correlation coefficient of the mean clutter level as well. Moreover, for each combination of the correlation coefficient, the clutter shape parameter and the *CNR* values the optimal number of reference cells exist that provides the best possible detection performance for a given *Pfa*, i.e. provides the lowest possible value of CFAR loss of the mean clutter plus noise level estimation.

As discussed in Section 3.2.2, the maximum possible values of CFAR gain (i.e. the minimum negative CFAR loss values) is given by the difference between the "ideal fixed" and "ideal CFAR" thresholds. For "ideal CFAR" performance, when the local mean clutter level is known exactly, the value of β will be fixed at that required for the speckle component of the clutter (i.e. Gaussian clutter, with the shape parameter $\nu = \infty$) and noise. The practical CFAR gain is likely to be significantly less than this theoretical limit as a typical CA CFAR processor does not adapt the detection threshold according to the local value of the correlation coefficient p and the local mean clutter level in the test cell is not estimated exactly.

According to the results presented in Table 8, substantial CFAR gains may be achieved in clutter-limited conditions only when the clutter spatial correlation length is longer than 5 range samples (R_{corr} >5) and the clutter is spiky (ν <5) [28].

Table 8: Typical values of CFAR gain for CFAR lengths 2N = 10 and 2N = 100, Pd = 0.5 and Pfa = 10^{-4}.

	CFAR gain, dB					
	R_{cor} =0		R_{cor} =10		R_{cor} =30	
	2*N*=10	2*N*=100	2*N*=10	2*N*=100	2*N*=10	2*N*=100
ν_{eff} = 0. 50	-5.0	-0.5	2.6	1.6	6.4	3.7
ν_{eff} = 1.0	-3.3	-0.4	2.3	1.2	4.5	3.4
ν_{eff} = 5.0	-2.6	-0.3	-0.6	0.4	0.1	1.4

Figure 19 illustrates the variation with range of different types of threshold in one scan (no pulse-to-pulse integration) for the clutter-limited detection region (*CNR* > 10dB). The clutter has a shape parameter of ν = 0.5 and the spatial correlation distance of R_{corr} = 30. The average *Pfa* is 10^{-4} and the threshold has been set to give a *Pd* of 0.5 for a Swerling 2 target in each case.
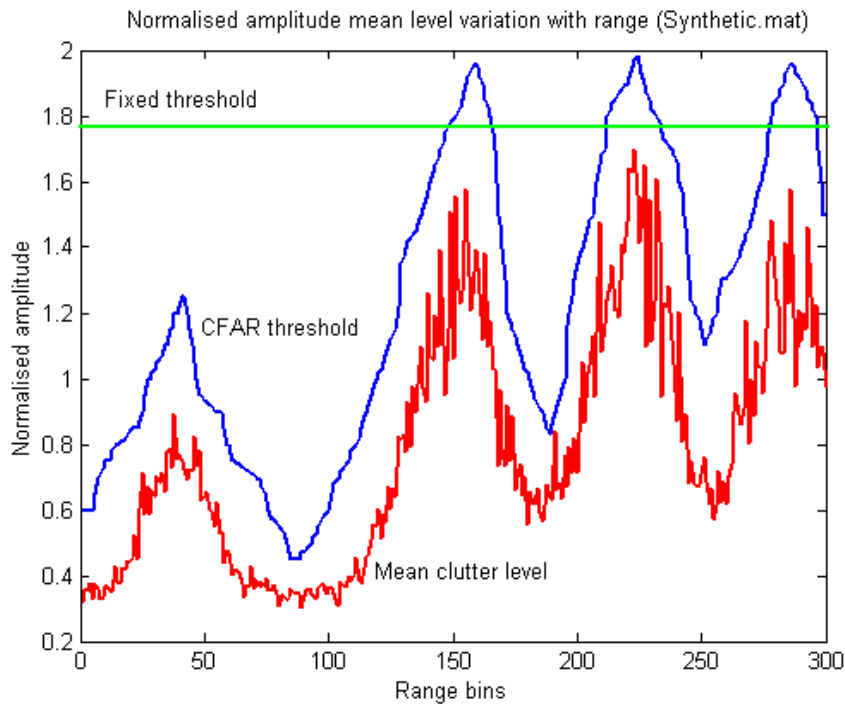
Figure 19: Variation of thresholds with range in strongly correlated K-distributed clutter
(R_{cor}= 30) with ν = 0.5 for average Pf a = 10^{-4} (red – mean clutter level for ν = 0.5
and $R_{cor\,r}$= 30; green – ideal fixed threshold; blue - average threshold for a double-
sided CA CFAR with N = 5 and G=1).

It can be seen that for the case when R_{corr} = 30, the average threshold of the 5+5 cell-average detector is significantly lower than that for the fixed threshold and so a detection gain is to be expected. Therefore, the substantial CFAR gains may be achieved when the clutter exhibits strong spatial correlation.

When the returns show a strong periodic spatial variation (normally associated with the sea swell), it may be possible to adapt to the local variations of mean level by using a cell-averaging length, which is shorter than the sea swell wavelength. As a number of reference cells 2*N* becomes large, performance tends to the CFAR loss associated with clutter with no spatial correlation.

It was shown that [28, 38]:

- For the case of strongly correlated sea clutter, the average false alarm rate for the fixed threshold is dominated by a localised area of high clutter, the CA CFAR gives a lower average threshold and much more even distribution of false alarms. The areas of highest false alarm rate are not in the region of high clutter return, but associated with more randomly distributed regions of rapidly changing clutter amplitude, and

- When the clutter exhibits strong spatial correlation, for low effective shape parameter values (ν_{eff} < 1) the best performance is nearly always achieved for a short cell-averager length.

Therefore, the CFAR processing design with a short cell-averaging length is optimal for the conditions of medium and high sea states in the clutter-limited and intermediate detection regions, when the sea is fully developed, or in the clutter-limited detection region of the non-equilibrium sea, when swell is observed. The use of shorter averaging lengths will enable the thresholds to follow more rapid spatial variations but will also introduce increased the CFAR loss due to fluctuations of the threshold induced by the speckle component of the clutter. Such short cell-averages will also produce the highest CFAR loss in uncorrelated clutter.

3.4.3 Additional CFAR Loss of the Mean Clutter Plus Noise Level Estimation Due to an Inappropriate Choice of the Gap Size

Another very important parameter of any CFAR processor design that strongly influences the accuracy of the mean clutter plus noise level estimation is the gap size. If a target is range extensive (i.e. a big ship), and it should be detected by a high-resolution radar mode that is optimised for the detection of small size targets, such as submarine periscopes, the gap size should be sufficient to prevent the target contaminating the threshold estimate as this may modify the CFAR gain or loss achieved. With a short gap, some of the target responses can be positioned in the nearest (from the cell under test) range samples used in the cell-averaging filter (see Figure 20). That would be a source of inaccurate (overestimation of) local mean clutter plus noise level estimation.
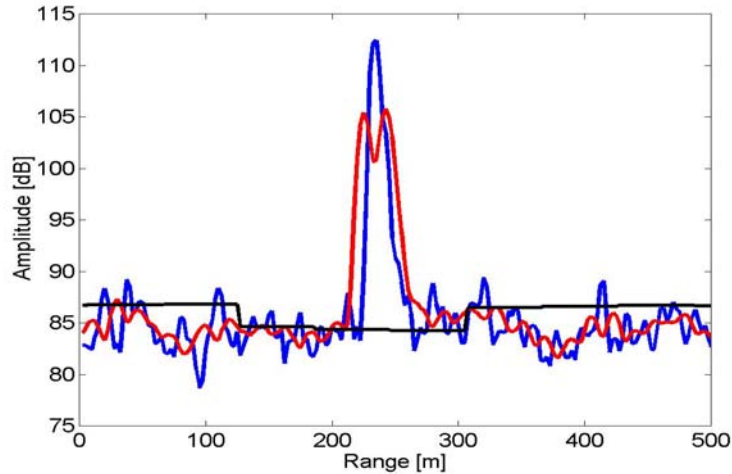
Figure 20: Influence of the chosen gap size on the accuracy of the mean clutter plus noise level estimation.

In Figure 20 a blue line presents a high-resolution range profile of sea clutter and target responses with a 35 m-long target positioned at the distance of 240 m; the red line shows variation with range of the local mean level estimate, produced by the CA CFAR processor with 2.5 m gap and 10 m reference window lengths; and the black line the variation with range of the global mean level estimate, produced by the CA CFAR processor with 60 m gap and 240 m reference window lengths. It can be seen that, due to an insufficient gap size, the CA CFAR processor with 2.5 m gap length produces a

wrong estimate of the mean clutter level around the target that could prevent successful target detection. At the same time, the CA CFAR processor with a 60 m gap length achieves much higher accuracy in the mean clutter level estimation around the target, and would detect the target with high probability. However, in strongly spatially correlated clutter the choice of a longer gap without the consideration of the clutter correlation distance can create problems because the local mean level around the cell under test can be estimated incorrectly.

For example, Figures 21 and 22 present the results of mean clutter plus noise level estimation using cell-averaging filters with the same number of reference window cells $2N$ =10. The clutter spatial correlation distance is 10 range cells. Figure 21 corresponds to the cell-averaging filter with the gap size equal to 1 range cell, Figure 22 corresponds to the cell-averaging filter with the gap size equal to 10 range cells. It can be seen that in strongly spatially correlated clutter the choice of a gap size of the order of clutter correlation distance provides the wrong estimate of mean clutter plus noise level. It results in an increased false alarm rate and an additional detection loss. For the reasons considered, it is clear that a high-resolution radar system must be able to adapt its cell-averaging window and gap lengths according to the sea conditions and a target size, if the best performance is to be achieved.

Figure 21: Variation of mean clutter plus noise estimate with range in strongly correlated K-distributed clutter (R_{cor}= 10) (red – clutter plus noise mixture range profile; blue - mean clutter plus noise level estimate for a double-sided CA CFAR with N=5 and G=1).
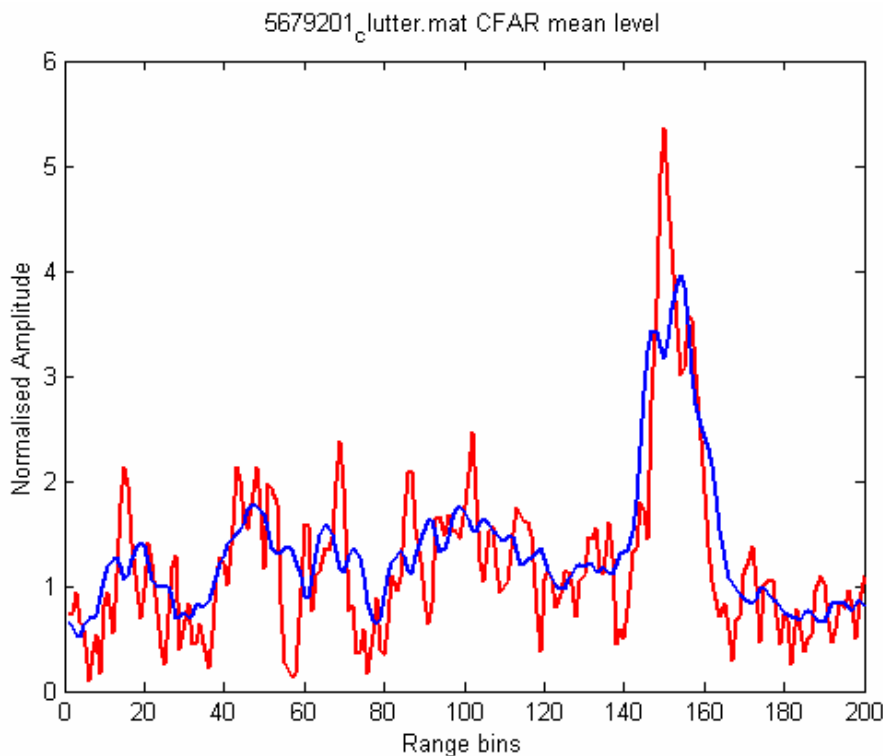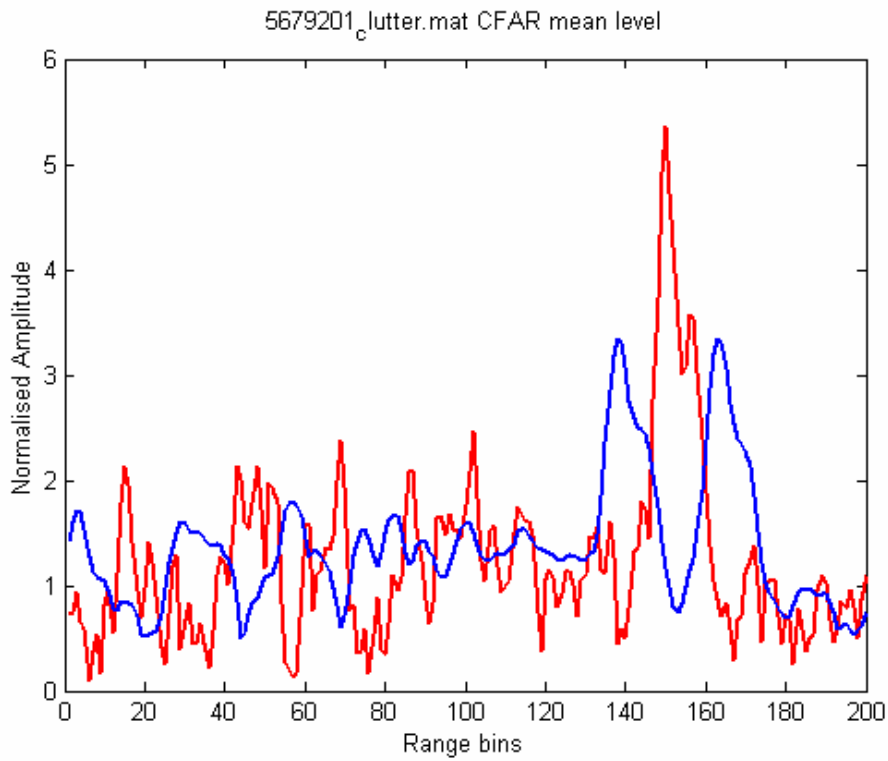
Figure 22: Variation of mean clutter plus noise estimate with range in strongly correlated K-distributed clutter (R_{cor}= 10) (red – clutter plus noise mixture range profile; blue – mean clutter plus noise level estimate for a double-sided CA CFAR with N=5 and G=10).

3.5 CFAR Loss of the Threshold Multiplier Estimation

Finally, there will be another source of CFAR loss in a high-resolution radar system. There will be errors in setting the appropriate value of the threshold multiplier, i.e. an additional CFAR loss due to the difference between the optimal and estimated threshold multipliers values.

3.5.1 Threshold Multiplier Estimation in Rayleigh Clutter plus Noise Mixture

It is well known that, if the amplitude of a clutter plus noise mixture is Rayleigh – distributed, only the mean clutter plus noise level needs to be estimated [2-4]. The threshold-multiplying factor value β is determined in this case only by the required *Pd*, *Pfa* and a Swerling target model. If the interference is noise-limited, and a CFAR detector estimates the threshold levels based upon the K-distribution, then the chosen CFAR threshold suffers a small CFAR loss (say, less than 0.5dB) due to the necessity of estimating the shape parameter ν.

3.5.2 Threshold Multiplier Estimation in Non-Rayleigh Clutter plus Noise Mixture

To estimate the appropriate value of the threshold multiplier in K-distributed clutter plus noise mixture, the shape parameter ν of the clutter component and *CNR* must also be determined additionally to the mean clutter plus noise level. Errors in estimation of the shape parameter ν and *CNR* will result in an incorrect value of the threshold multiplier being used, causing degradation in the detection performance:

- If the threshold is set too high (ν is estimated too low and/or *CNR* is estimated too high), the consequence will be an increased detection loss.
- If the threshold is set too low (ν is estimated too high and/or *CNR* is estimated too low), the consequence will be an increased false alarm probability.

The appropriate magnitude of the CFAR loss of the threshold multiplier, L_{THR}, estimation associated with ν being underestimated and/or *CNR* being overestimated is obtained as the difference between the required *S(C+N)R* determined for given *Pfa* and *Pd* for a CFAR detector with the specified number of reference cells 2*N*, which detect a Swerling 2 target in K-distributed clutter and noise mixture with the estimated values of ν and *CNR*, and with the true values of these parameters, when the clutter correlation length is equal to R_{corr} range samples

$$L_{THR} \;=\; S(C+N)R_{req}\left[\hat{\nu}, CNR_{est}, 2N, R_{cor}\right] - S(C+N)R_{req}\left[\nu, CNR, 2N, R_{corr}\right], \quad (3.110)$$

A good approximation to L_{THR} is given by the difference of the required threshold multiplier values for a CFAR detector with the specified number of reference cells 2*N* to keep the required false alarm rate in conditions of K-distributed clutter plus noise mixture with the estimated values ν and *CNR*, and with the true values of these parameters, when the clutter correlation length is equal to R_{corr} range samples

$$\beta_{THR} \;=\; \beta\left(\hat{\nu}, CNR_{est}, 2N, R_{corr}\right) - \beta\left(\nu, CNR, 2N, R_{corr}\right) \qquad (3.111)$$

Under most operational conditions, however, the performance degradation due to ν being estimated too high and/or the *CNR* being estimated too low will be of more interest in that it may cause a notable increase in *Pfa*.

Determine the value of β_{THR} for this case as follows.

Due to errors in estimation of the shape parameter ν and the *CNR*, the achieved *Pfa*, $\overline{P_{fa}^{\,CFAR}}$, increases compared to the required *Pfa*, $\overline{P_{fa}^{\,REQ}}$, as

$$\overline{P_{fa}^{\,CFAR}} \;=\; \overline{P_{fa}^{\,REQ}} \;+\; \Delta\overline{P_{fa}}\,. \qquad (3.112)$$

To counter this increase, the design *Pfa* must be reduced to

$$\overline{P_{fa}^{DESIGN}} = \frac{\overline{P_{fa}^{REQ}}}{1 + \dfrac{\Delta \overline{P_{fa}}}{P_{fa}^{REQ}}}, \tag{3.113}$$

in order to constrain Pfa to $\overline{P_{fa}^{REQ}}$, at worst.

If the threshold multiplier β_{DESIGN} is required to achieve $\overline{P_{fa}^{DESIGN}}$, and the threshold multiplier β_{REQ} to achieve $\overline{P_{fa}^{REQ}}$, then their difference is approximately the CFAR loss of the threshold multiplier estimation

$$L_{THR} \approx \beta_{THR} = \beta_{DESIGN} - \beta_{REQ}. \tag{3.114}$$

As an example, Table 9 presents the approximate values for the increased Pfa as a function of the true and estimated values of the shape parameter of spatially uncorrelated sea clutter, for the CA CFAR processor with $2N = 32$ reference cells and a nominal $\overline{P_{fa}} = 10^{-6}$.

Table 9: Increased Pfa due to errors in estimation of the spatially uncorrelated clutter shape parameter for the CA CFAR processor with 32 reference cells and a nominal Pfa=10^{-6}.

$\nu_{estimated}$	ν_{true}		
	$0.75\ \nu_{estimated}$	$0.5\ \nu_{estimated}$	$0.25\ \nu_{estimated}$
10	$10^{-5.5}$	$10^{-5.0}$	$10^{-4.2}$
2	$10^{-5.2}$	$10^{-4.5}$	$10^{-3.3}$
5	$10^{-5.0}$	$10^{-4.0}$	$10^{-2.5}$

For a different number of reference cells and other types of CFAR processors (GO and SO), the results are not notably different [14].

It can be shown that in spatially uncorrelated K-distributed clutter [14]:

- All three types of CFAR processor considered (CA, GO and SO) are approximately equally sensitive to errors in the estimated values of ν and *CNR*.

- The number of reference cells used in forming the test statistic does not significantly influence the sensitivity of the CFAR processors to errors in the estimated values of ν and *CNR*.

- All three types of CFAR processor considered, (CA, GO and SO) are more sensitive to errors in the estimated value of ν and *CNR* for low false alarm rates than for higher false alarm rates.

- All three types of CFAR processor considered (CA, GO and SO) are more sensitive to errors in the estimated values of v and *CNR* for small values of the clutter shape parameter than for large values.

Figure 23 presents the calculated CFAR loss of the threshold multiplier estimation due to errors in estimation of the shape parameter of uncorrelated sea clutter, when $v_{estimated} = 1.5 v_{true}$ and a nominal $Pfa = 10^{-6}$. It can be seen that the smaller the shape parameter value, the larger the CFAR loss value.

In spatially correlated K-distributed clutter for a given degree of correlation, the spikier the clutter, the lower the required value of *Pfa*, and the higher the required value of *Pd*, the nearer the CFAR loss lies to the completely uncorrelated case [14].
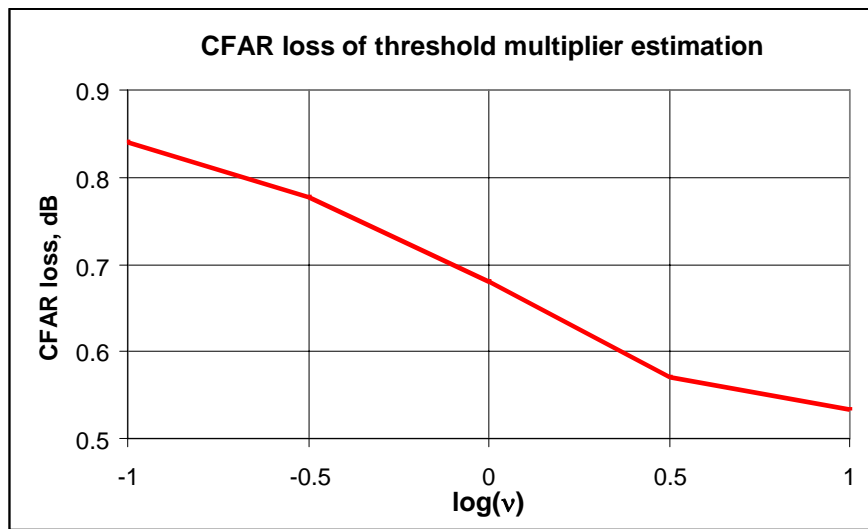
Figure 23: CFAR loss of the threshold multiplier estimation due to errors in estimation of the shape parameter of clutter, when $v_{estimated} = 1.5 v_{true}$ and a nominal Pfa=10^{-6}.

Consider now the accuracy of different methods for estimation of the shape parameter v and *CNR* in conditions of non-Rayleigh background with different spatial correlation properties.

If a sufficiently large number of independent samples of clutter plus noise mixture are available to estimate the higher moments of the clutter plus noise amplitude PDF accurately, the shape parameter v of the clutter component and *CNR* can be estimated by matching second, fourth and sixth moments of the data to their theoretical values [27].

Then:

$$v = \frac{18 \left(m_4 - 2 m_2^2 \right)^3}{\left(12 m_2^3 - 9 m_2 m_4 + m_6 \right)^2} , \qquad (3.115)$$

$$CNR = \frac{2v}{\pi\, b^2\, \sigma^2}, \tag{3.116}$$

where:

$$2\sigma^2 = m_2 - \left[\frac{v}{2}\left(m_4 - 2m_2^2\right)\right]^{\frac{1}{2}}, \tag{3.117}$$

$$b^2 = \frac{4v}{\pi\left(m_2 - 2\sigma^2\right)}, \tag{3.118}$$

$$m_k = \frac{1}{2N}\sum_{i=1}^{2N}\left(w_i - \bar{z}\right)^k. \tag{3.119}$$

However, the accuracy of the higher order estimates is likely to be poor unless the sample size is very large, and the CFAR loss of the threshold multiplier estimation value is large.

A good estimate of the *CNR* at a given range for a radar system with the automatic gain control (AGC) is given by [33]

$$CNR = \frac{G_N}{G_C}, \tag{3.120}$$

where G_N is the AGC gain demand in noise, determined between pulses or at maximum range, and G_C is the AGC gain demand in local clutter.

It was shown [36] that a close approximation to the maximum likelihood (ML) estimate of v in the presence of thermal noise is based on the estimates of the mean clutter plus noise intensity $\bar{z}$ and the logarithm of the data, $\overline{\log_e(w)} = \frac{1}{2N}\sum_{i=1}^{2N}\log_e(w_i)$. For single pulse detection in each scan it is given as

$$\log_e(\hat{v}) - \Psi(\hat{v}) = \log_e(\bar{z}) - \overline{\log_e(w)} + \Psi(1) + \csc(\pi v)\,\pi\,(-1)^v\left[1 - \frac{\gamma\left(v, -v/CNR\right)}{\Gamma(v)}\right] +$$

$$\frac{v}{(v-1)CNR}\,_2F_2\left[1,1;2,2-v;v/CNR\right], \tag{3.121}$$

where $\Psi(a)$ is the digamma function, $\gamma(a,b)$ is the incomplete Gamma function, and $_2F_2$ is the hypergeometric function.

The equation (3.121) is not very convenient for practical application and it should be noted that it is not analytic for integer values of ν, which have to be calculated separately.

If the *CNR* cannot be estimated directly, an alternative method can be used to determine the appropriate value of the threshold multiplier β. As discussed in Section 3.1, the estimation of *Pfa* requires an estimate of the CDF of clutter plus noise in the "tail" of the distribution. It can be shown that the tail of the distribution of K-distributed clutter plus noise can be fitted to a K-distribution with a different shape parameter, ν_1 [27]. The estimate of ν_1 is obtained by using a method of estimating a shape parameter of clutter, when the influence of noise can be neglected, such as:

- Method based on the arithmetic and geometric means estimation, proposed by Raghavan [34], that uses the similarity between the K and Gamma-distributions,

- Method based on the first and second amplitude sample moments estimation (FSM), proposed in [34],

- Method based on the second and fourth amplitude sample moments estimation, proposed by Watts [27],

- Method based on the estimates of the mean intensity and the mean of the logarithm of the data [36], and

- Method based on the estimates of the mean intensity and the variance of the logarithm of the data [36].

It was shown [36] that the best results in the clutter-limited conditions, when the influence of noise can be neglected, are achieved by using a method, which is based on the estimates of the mean intensity $\bar{z}$ and the mean of the logarithm of the data, $\overline{\log_e(w)} = \dfrac{1}{2N}\displaystyle\sum_{i=1}^{2N}\log_e(w_i)$, and which is presented for single pulse detection in each scan as

$$\log_e\left(\hat{\nu}_1\right) - \Psi\left(\hat{\nu}\right) \;=\; \log_e\left(\bar{z}\right) - \overline{\log_e\left(w\right)} + \Psi\left(1\right), \qquad\qquad 3.122)$$

Given the value of $\hat{\nu}_1$ determined from (3.122), the value of the threshold multiplier for fixed threshold detection is obtained from

$$P_{fa} \;\approx\; \frac{2}{\Gamma\left(\hat{\nu}_1\right)}\left(\frac{t_{ideal\ fixed}\,\hat{\nu}_1}{\bar{z}}\right)^{\hat{\nu}_1/2} K_\nu\left(2\sqrt{\frac{t_{ideal\ fixed}\,\hat{\nu}_1}{\bar{z}}}\right) \;=\; \frac{2}{\Gamma\left(\hat{\nu}_1\right)}\left(\beta_{ideal\ fixed}\,\hat{\nu}_1\right)^{\hat{\nu}_1/2} K_{\hat{\nu}_1}\left(2\sqrt{\beta_{ideal\ fixed}\,\hat{\nu}_1}\right)$$

$$(3.123)$$

Then the value of the threshold multiplier for a CA CFAR detector with the specified number of reference cell *2N* that provides the required *Pfa* in clutter with the shape parameter $\hat{\nu}_1$ and correlation length R_{corr} is given by (3.102).

However, this method gives a very poor fit to the tail of the amplitude PDF of clutter plus noise mixture, when the influence of noise cannot be neglected. This is illustrated in Figure 24, which shows the CDF for $v = 0.1$ and $CNR = 0\text{dB}$.
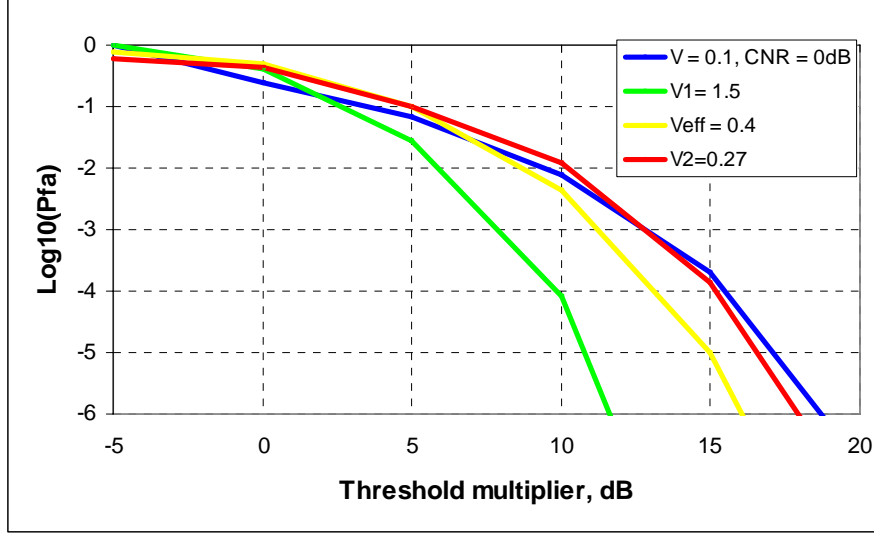

Figure 24: Comparison of clutter plus noise CDF with different estimates of the K-distribution in spatially uncorrelated sea clutter plus noise mixture.

Application of equation (3.116) in a Monte Carlo simulation using 10 000 independent samples gave an estimate for v of $\hat{v}_1 = 1.5$. It can be seen that the CDF for $\hat{v}_1 = 1.5$ provides a very poor fit to the tail of the CDF for $v = 0.1$ and $CNR = 0\text{dB}$.

As discussed in [27], a comparison of moments of the distribution of the clutter and clutter plus noise mixture suggests an effective value of v given by

$$v_{eff} = \left[\frac{m_4}{2m_2^2} - 1 \right]^{-1} = v \left(1 + \frac{1}{CNR} \right)^2 . \qquad (3.124)$$

This method provides a more accurate fit to the tail of the CDF for $v = 0.1$ and $CNR = 0\text{dB}$, as it is also shown in Figure 24, even the value of $v_{eff} = 0.4$ still overestimates v. If noise is taken into account, then the effective value v_{eff} must be replaced by the true value v, when setting the threshold value

$$v = \frac{v_{eff}}{\left(1 + \frac{1}{CNR} \right)^2} . \qquad (3.125)$$

A better method is to make a fit to the tail of the CDF of the data by direct comparison of distribution functions [13, 38]. Obtaining an exact match at $Pfa = 10^{-3}$ gives

$\hat{v}_2 = 0.27$, which is also shown in Figure 24 and is the best fit of the three considered estimates.

Once a fit to the tail has been achieved, the distribution can be extrapolated to predict the threshold values required for lower values of *Pfa*. An indication of the accuracy that can be achieved by fitting to the tail of the CDF is summarised in Table 10 for 10 pulses integrated prior to CFAR processing and 1000 independent samples used to estimate the distribution. (The choice of 1000 data points is representative for the range extent of clutter returns from real radars for which the clutter statistics may be considered constant).

Table 10: Mean and standard deviation of estimates of ν matching to the tail of the distribution using 1000 independent samples.

ν	Mean $\hat{v}$	Standard deviation $\hat{v}$
10	10.11	2.22
1	1.02	0.10
0.5	0.52	0.06

A variation of $\pm\,\sigma$ in $\hat{v}$ of the magnitudes shown for direct matching to the tail of the distribution, where σ is the standard deviation of $\hat{v}$, is equivalent to a CFAR loss of about $\pm\,0.5$dB in the threshold multiplier β.

The results presented in Table 10 on the standard deviation of the K-distribution shape parameter estimators assume that the clutter samples are spatially uncorrelated. When the samples are correlated, the standard deviation of the estimates will be larger than is indicated by the same number of samples for an uncorrelated case. Consequently, more samples are required in the correlated case than the uncorrelated case to achieve the same standard deviation on the estimators.

4. Summary

The report addresses the problem of CFAR processing loss estimation for a high-resolution maritime surveillance radar system with a generic ASW mode.

It was shown that the CFAR loss for any high-resolution system CFAR processor design, as measured by the change in *S(C+N)R* required to maintain *Pd* for a given *Pfa*, can vary widely over the area of operation of the radar and is a function of the following parameters:

- When clutter plus noise mixture is spatially uncorrelated and Rayleigh-distributed, for any type of a CFAR detector the CFAR loss is a function of *Pfa*, *Pd*, the target model, the cell-averaging length and the number of pulses integrated prior to CFAR processing.

- When clutter plus noise mixture is spatially uncorrelated or weakly correlated, and has a non-Rayleigh distribution, the CFAR loss is additionally a function of the shape parameter and the *CNR*.

- When clutter plus noise mixture is strongly spatially correlated and non-Rayleigh-distributed, the interaction between the cell-averaging CFAR processor and clutter theoretically can produce a CFAR gain. The highest values of CFAR gain are achieved with a short cell-average filter length in highly spatially correlated clutter. However, such short cell-averager filters will also produce the highest CFAR loss in uncorrelated clutter and noise-limited conditions.

Thus, a simple achievable CFAR processing accuracy measure such as the CFAR loss value that is given by a single number for all detection regions, as it is usually done for a low-resolution radar system, is not sufficient to describe the CFAR processing loss of a high-resolution radar system expected in a complex environment.

The CFAR processing loss for a high-resolution radar system must be quantified for different detection regions and for a number of levels of complexity:

- The CFAR loss in noise-limited detection region;

- The CFAR loss in uniform clutter with changing scale and amplitude statistics (shape);

- The CFAR loss in non-uniform clutter with specified spatial characteristics (spatially correlated returns from sea swell etc).

5. References

1. Antipov, I., Baldwinson, J., "Detection Performance Prediction Model for a Generic Anti-Submarine Warfare Radar Mode", DSTO-TR-1101, pp. 82, 2001.

2. Barton, D., "Modern Radar System Analysis", Artech House, 1988.

3. Barton, D.K., Leonov, S.A., "Radar Technology Encyclopedia", Artech House, 1997.

4. Skolink, M., Radar Handbook, 2nd Ed., McGraw-Hill, 1990.

5. Hansen, V.G., Sawyers, J.H., "Detectability Loss Due to "Greatest of" Selection in a Cell-Averaging CFAR", IEEE Trans. AES, Vol. AES-16, No 1,Jan. 1980, pp.115-118.

6. Moore, J.D., Lawrence, N.B., "Comparison of Two CFAR Methods Used with Square Law Detection of Swerling I Targets", IEEE International Conference, Proc., 1980, pp.403-409.

7. Weiss, M., "Analysis of Some Modified Cell-Averaging CFAR Processors in Multiple-Target Situations", IEEE Trans. AES, Vol. AES-18, No 1,Jan. 1982, pp.102-114.

8. De Miguel, G., Casar, J.R., "CFAR detection for Weibull and Other Log-log-linear Tail Clutter Distributions", IEE Proc.-Radar, Sonar, Navig., Vol. 144, No 2, 1997, pp. 64-70.

9. Farina, A., Studer, F.A., "A Review of CFAR Detection Techniques in Radar Systems", Microwave J., September 1986, pp. 115-128.

10. Bucciarelli, T., "CFAR Problems in a Non-Gaussian Clutter Environment", IRSI 83 Processing, 1983, pp. 333-338.

11. Hou, X.-Y., Morinaga, N., "Detection Performance in K-distributed and Correlated Rayleigh Clutters", IEEE Trans. AES, Vol. AES-25, No 5, 1989, pp.634-641.

12. Watts, S., Ward, K.D., "Spatial Correlation in K-distributed Sea Clutter", IEE Proc.-Radar, Sonar, Navig., Vol. 134, No 6, 1987, pp. 526-532.

13. Watts, S., "The Performance of Cell-averaging CFAR System in Sea Clutter", Proceedings of the IEEE International Radar Conference, 2000, pp. 398 -403.

14. Armstrong, B.C., Griffiths, H.D., "CFAR Detection of Fluctuating Targets in Spatially Correlated K-distributed Clutter", IEE Proceedings, Vol. 138, Pt F, No 2, April 1991, pp. 139-152.

15. Himonas, S.D., Barkat, M., "Adaptive CFAR Detection in Partially Correlated Clutter", IEE Proceedings, Vol. 137, Pt F, No 5, October 1990, pp. 387-394.

16. Barkat, M., Soltani, F., "Cell-averaging CFAR Detection in Compound Clutter with Spatially Correlated Texture and Speckle", IEE Proc.-Radar, Sonar, Navig., Vol. 145, No 6, December 1999, pp. 279-284.

17. Gandhi, P.P., Kassam, S.A.," Analysis of CFAR Processors in Nonhomogeneous Background", IEEE Trans. AES, Vol. AES-24, No 4, 1988, pp.427-445.

18. Nitzberg, R., "Composite CFAR Techniques", Proceedings of the IEEE International Radar Conference, 1993, IEEE Publication, pp. 1133-1137.

19. Smith, M.K., Varshney, P.K., "Intelligent CFAR Processor Based on Data Variability", IEEE Trans. AES, Vol. AES-36, No 3, 2000, pp.837-847.

20. Conte, E., Longo, M., Lops, M., "Performance Analysis of CA-CFAR in the Presence of Compound Gaussian Clutter", Electronic Letters, Vol. 24, No 13, 1988, pp.782-783.

21. Raghavan, R.S., "A Model for Spatially Correlated Radar Clutter", IEEE Trans. AES, Vol. AES-27, No 2, 1991, pp.268-275.

22. Marier, I.J., "Correlated K-distributed Clutter Generation for Radar Detection and Track", IEEE Trans. AES, Vol. AES-31, No 2, 1995, pp.568-580.

23. Armstrong, B.C., Griffiths, H.D., "Improved CFAR Detection in Spatially Correlated K-distributed Clutter", Proceedings of CIE, International Conference on Radar, 1991, pp.415-418.

24. Watts, S., Baker, C., Ward, K., "Maritime Surveillance Radar Part 2: Detection performance prediction in sea clutter", IEE Proceedings, Vol 137, Pt F, No 2, April 1990, pp. 63-72.

25. Ward, K.D., Baker, C.J., Watts, S., "Maritime Surveillance Radar. Part 1: Radar Scattering from the Ocean Surface", IEE Proc., Vol. 137, Pt. F, No 2, pp. 51-62, 1990.

26. Watts, S., "Radar Detection Prediction in Sea Clutter Using the Compound K-distribution Model", IEE Proceedings, Vol. 132, Pt F, No 7, December 1985, pp. 613-620.

27. Watts, S., "Radar Detection Prediction in K-Distributed Sea Clutter and Thermal Noise", IEEE Trans. AES, Vol. AES-23, No 1, Jan. 1987, pp. 40-45.

28. Watts, S., "Cell-averaging CFAR Gain in Spatially Correlated K-distributed Clutter", IEE Proc.-Radar, Sonar, Navig., Vol. 143, No 5, October 1996, pp. 321-327.

29. Antipov, I., "Simulation of Sea Clutter Returns", DSTO-TR-0679, pp. 58, 1998.

30. Watts, S., Wicks, D., "Empirical Models for Detection Prediction in K-Distribution Sea Clutter", IEEE Radar Conference, 1990, pp. 189 -194.

31. Denny, W.M., "K-distributed Sea Clutter: Performance Prediction Made Easy", IEE International Conference Radar-97, 14-16 October 1997, IEE Publication No.449, pp. 209 -213.

32. Watts, S., "Performance Measures for Airborne Maritime Surveillance Radars", IEE Colloquium on "Specifying and measuring performance of modern radar systems", 6th March 1998.

33. Watts, S., Gordon, A.J., "The Searchwater Family of Airborne Radars", IEE International Conference Radar-97, 14-16 October 1997, IEE Publication No.449, pp. 334 -338.

34. Raghavan, R.S.,"A Method for Estimating Parameters of K-distributed Clutter", IEEE Trans, AES, Vol. 27, No 2, pp. 238-246, 1991.

35. Joughin, I.R., Percival, D.B., Winebrenner, D.P., "Maximum Likelihood Estimation of K-distribution Parameters for SAR data", IEEE Trans. Geosci. Remote Sensing, Vol. 31, pp. 989-999, 1993.

36. Blacknell, D., "Comparison of Parameter Estimators for K-distribution", IEE Proc., Vol. 141, No 1, pp. 45-52, 1994.

37. Lombardo, P., Oliver, C.J., Tough, R.J.A., "Effect of Noise on Order Parameter Estimation for K-distributed Clutter", IEE Proc.-Radar, Sonar, Navig., Vol. 142, No 1, February 1995, pp. 33-40.

38. Watts, S., "Radar Performance in K-distributed Sea Clutter", RTO SET Symposium "Low Grazing Angle Clutter: Its Characterisation, Measurement and Application", RTO MP-60, pp. 372-379, April, 2000.

39. Denny, W.M., "K-distributed Sea Clutter: Small Target Processing", IEE International Conference Radar-97, 14-16 October 1997, IEE Publication No.449, pp. 591 -595.

40. Armstrong, B.C., Griffiths, H.D., "Modelling Spatially Correlated K-distributed Clutter", Electronic Letters, Vol. 27, No 15, 1991, pp.1355-1356.

41. Tonkin, S.P., Dolman, D.L., "Sea Surface Effects on the Radar Return from a Periscope", IEE Proceedings, Vol. 137, Pt F, No 2, April 1990, pp. 149-156.

42. Ward, K.D., Tough, R.J.A., "Radar detection Performance in Sea Clutter with Discrete Spikes", pp. 5, IEE Radar 2002 Proceedings.

43. Watts, S., Stove, A. G., "Non-Coherent Integration Strategies In Scanning Radar For The Detection Of Targets In Sea Clutter And Noise", International Radar Conference Radar 2004, Toulouse 19-21 October 2004.

44. Watts, S., Knight, G., "Performance Prediction for Scanning Radars with Correlated Returns from K-distributed Sea Clutter", International Radar Conference Radar 2004, Toulouse 19-21 October 2004.

45. Ward, K.D., Tough, R.J.A., Watts, S., "The Physics and Modelling of Discrete Spikes in Radar Sea Clutter", International Radar Conference Radar 2005, Toulouse 9-12 May, 2005.

46. Ward, K.D., Tough, R.J.A., Watts, S., "Sea clutter: Scattering, the K distribution and Radar Performance", IET Radar, Sonar and Navigation, Series 20, 2006.

47. Ward, K.D., Tough, R.J.A., Watts, S., "Modelling Sea Clutter Temporal Correlation in Detection Calculations", pp. 4, IET International Conference of Radar Systems, Radar 2007 Proceedings, Edinburgh, 15-18 October 2007.

48. Ward, K.D., Tough, R.J.A., Watts, S., "CFAR Loss and Gain in K-distributed Sea-Clutter and Thermal Noise", pp. 5, IET International Conference of Radar Systems, Radar 2007 Proceedings, Edinburgh, 15-18 October 2007.

DEFENCE SCIENCE AND TECHNOLOGY ORGANISATION DOCUMENT CONTROL DATA		1. PRIVACY MARKING/CAVEAT (OF DOCUMENT)
2. TITLE Estimation of a Constant False Alarm Rate Processing Loss for a High-Resolution Maritime Radar System		3. SECURITY CLASSIFICATION (FOR UNCLASSIFIED REPORTS THAT ARE LIMITED RELEASE USE (L) NEXT TO DOCUMENT CLASSIFICATION) Document (U) Title (U) Abstract (U)

4. AUTHOR(S) Irina Antipov and John Baldwinson	5. CORPORATE AUTHOR Defence Science and Technology Organisation PO Box 1500 Edinburgh SA 5111 AUSTRALIA

6a. DSTO NUMBER DSTO-TR-2158	6b. AR NUMBER AR-014-236	6c. TYPE OF REPORT Technical Report	7. DOCUMENT DATE August 2008

8. FILE NUMBER (U) 9505-23-50	9. TASK NUMBER NAV 07/58	10. TASK SPONSOR DGNAVSYS	11. NO. OF PAGES 78	12. NO. OF REFERENCES 48

13. URL on the World Wide Web http://www.dsto.defence.gov.au/corporate/reports/DSTO-TR-2158.pdf	14. RELEASE AUTHORITY Chief, Electronic Warfare and Radar Division

15. SECONDARY RELEASE STATEMENT OF THIS DOCUMENT

Approved for Public Release

OVERSEAS ENQUIRIES OUTSIDE STATED LIMITATIONS SHOULD BE REFERRED TO DOCUMENT EXCHANGE, PO BOX 1500, EDINBURGH, SA 5111, AUSTRALIA

16. DELIBERATE ANNOUNCEMENT

No Limitations

17. CASUAL ANNOUNCEMENT	Yes

18. DSTO RESEARCH LIBRARY THESAURUS

Sea clutter, detection performance, high-resolution radar system

19. ABSTRACT

This report addresses a problem of estimation of a constant false alarm rate (CFAR) processing loss for a high-resolution maritime radar system on an example of a generic radar system Anti-Submarine Warfare mode and discusses approaches to modelling of the detection performance for such a system. It has been shown that the value of the CFAR loss for a high-resolution radar system can vary considerably over a radar detection range, dependent on the clutter scenario and the CFAR detection processing used and, therefore, can not be given by a single number for the whole detection area, as it is usually done for a low-resolution radar system.